MOTOROLA

ACCREDITED

TESTING CERT # 2518.01

FCC ID: AZ492FT3821
DECLARATION OF COMPLIANCE: MPE ASSESSMENT

Government & Public Safety
EME Test Laboratory
8000 West Sunrise Blvd
Fort Lauderdale, FL. 33322

Date of Report: 6/18/2008
Report Revision: O
Report ID: SR6380_MPE rpt_APX7500_VHF_ Mobile_Rev O_080618

Responsible Engineer:	Kim Uong (Principal Staff EME Test Engineer)
Date/s Tested:	4/28/08-6/5/08
Manufacturer/Location:	Motorola Schaumburg, IL
Date submitted for test:	4/24/08
DUT Description:	APX7500 Single Band VHF 100W, 136 - 174 MHz
Test TX mode(s):	CW
Max. Power output:	120 Watts
TX Frequency Bands:	136-174MHz
Signaling type:	Analog, APCO 25, and TDMA (F2)
Model(s) Tested	M30KTS9PW1AN
Model(s) Certified:	M30KTS9PW1AN
Serial Number(s):	83
Classification:	Occupational/Controlled Environment
Rule Part(s):	22 and 90

DUT Photo
(Refer to Exhibit 7B)

Approved Accessories:
Antenna(s):
HAD4006A (Roof Mount 136 - 144 MHz, 1/4 Wave, 2.15dBi)
HAD4007A (Roof Mount 144-150.8 MHz, 1/4 Wave, 2.15dBi)
HAD4008A (Roof Mount 150.8-162 MHz, 1/4 Wave, 2.15dBi)
HAD4009A (Roof Mount 162 - 174 MHz, 1/4 Wave, 2.15dBi)
RAD4010ARB (Thru-hole Mount 136 - 174 MHz, 1/2 Wave, 5.15dBi)
HAD4016A (Roof Mount 136 - 162 MHz, 1/4 Wave, 2.15dBi)
HAD4017A (Roof Mount 146 - 174 MHz, 1/4 Wave, 2.15dBi)
HAD4021A (Roof Mount 136 - 174 MHz, 1/4 Wave, 2.15dBi)

Final RF Exposure Results:
Max. Calc. : 1-g Avg. SAR: 0.813 W/kg;

Based on the information and the testing results provided herein, the undersigned certifies that when used as stated in the operating instructions supplied, said product complies with the national and international reference standards and guidelines listed in section 3.0 of this report. This report shall not be reproduced without written approval from an officially designated representative of the Motorola EME Laboratory.
I attest to the accuracy of the data and assume full responsibility for the completeness of these measurements.
This reporting format is consistent with the suggested guidelines of the TIA TSB-159 April 2006
The results and statements contained in this report pertain only to the device(s) evaluated herein.

Signature on file - Deanna Zakharia

Deanna Zakharia G&PS EME Lab Senior Resource Manager, Laboratory Director,

Approval Date: 6/26/08

Certification Date: 6/26/08

Certification No.: L1080618P

TABLE OF CONTENTS

1.0 Product and System Description

2.0 Additional Options and Accessories

3.0 Measurement and Limit Standards

4.0 Measurement System Uncertainty Levels

5.0 Method of Measurement

- 5.1 EME measurements made with trunk mounted antenna
  - 5.1.1 External/Bystander vehicle EME measurement
  - 5.1.2 Internal/Passenger vehicle EME measurement
- 5.2 EME measurements made with roof mounted antenna
  - 5.2.1 External/Bystander vehicle EME measurements
  - 5.2.2 Internal/Passenger vehicle EME measurement

6.0 Test Site

7.0 Measurement System/Equipment

8.0 DUT Output Power

9.0 Test Set-Up Description

10.0 Test Results Summary

11.0 Conclusion

APPENDIX A: Illustration of Antenna Location and Test Distances
APPENDIX B: Meter/Probe Calibration Certificates
APPENDIX C: DUT Photos
APPENDIX D: SAR Simulation Report

REVISION HISTORY

Date	Revision	Comments
6/18/2008	O	Initial release

1.0 Product and System Description

FCC ID: AZ492FT3821, model M30KTS9PW1AN is a mobile transceiver that utilizes analog, APCO 25 & F2 digital two-way radio communications. The analog modulation scheme uses Frequency Modulation (FM). APCO 25 & F2 digital modes use C4FM of CQPSK family of modulation (Compatible 4-Level Frequency Modulation of Compatible Quadrature Phase Shift Keying). F2 is a TDMA protocol that allocates portions of the RF signal by dividing time into two slots (2 slots TDMA). Transmission from a unit or base station is accommodated in time-slot lengths of 30 milliseconds and frame lengths of 60 milliseconds. This product supports voice in analog mode, and both voice and data modes in digital mode.

The maximum duty cycle for analog mode is 50%. The APCO mode is based on simplex hand-shaking operation between the user and base station. The maximum duty cycle for F2 protocol is 50% which controlled by the software as defined in the protocol.

The intended use of the radio is Push-To-Talk (PTT) while the device is properly installed in a vehicle with an external antenna mounted at the center of the roof or trunk.

This device will be marketed to and used by employees solely for work-related operations, such as public safety agencies, e.g. police, fire and emergency medical. User training is the responsibility of these agencies which can be expected to employ the usage instructions, safety information and operational cautions set forth in the user's manual, instructional sessions or other means.

Accordingly this product is classified as Occupational/Controlled Exposure. However, in accordance with FCC requirements, the passengers inside the vehicle and the bystanders external to the vehicle are evaluated to the General Population/Uncontrolled Exposure Limits.

(Note that “Bystanders” as used herein mean people other than operator)

2.0 Additional Options and Accessories

NA

3.0 Measurement and Limit Standards

Measurements were performed according to the recommended guidelines in IEEE/ANSI C95.3-2002 and compared to FCC Limits Per 47 CFR 2.1091 (d) for General Population/ Uncontrolled RF Exposure.

For test frequencies ranging from 136 - 174MHz the MPE (Maximum Permissible Exposure) limit to electromagnetic energy in equivalent plane wave free-space power density is 0.2mW/cm^2.

4.0 Measurement System Uncertainty Levels

Uncertainty Budget for Near Field Probe Measurements

	Tol. (± %)	Prob. Dist.	Divisor	u_i (±%)	v_i
Measurement System					
Probe Calibration	6.0	N	1.00	6.0	∞
Survey Meter Calibration	3.0	N	1.00	3.0	∞
Hemispherical Isotropy	8.0	R	1.73	4.6	∞
Linearity	5.0	R	1.73	2.9	∞
Pulse Response	1.0	R	1.73	0.6	∞
RF Ambient Noise	3.0	R	1.73	1.7	∞
RF Reflections	8.0	R	1.73	4.6	∞
Probe Positioning	10.0	R	1.73	5.8	∞
Test sample Related					
Antenna Positioning	3.0	N	1.00	3.0	∞
Power drift	5.0	R	1.73	2.9	∞
Combined Standard		RSS		12.2	∞
Expanded Uncertainty (95% CONFIDENCE LEVEL)		k=2		24	

FCD-1770, Rev. 1

5.0 Method of Measurement

5.1 EME measurements made with trunk mounted antenna(s)

(Refer to APPENDIX A for antenna location and test distances)

5.1.1 External/Bystander vehicle EME measurement

(Antenna mounted at trunk center)

MPE measurements for bystander conditions are determined by taking the average of (10) measurements in a 2m vertical line for each of the (3) test locations indicated in appendix A with 20cm increments at the test distance of 90cm from the antenna under test. The measurement probe is positioned orthogonal to antenna (typically parallel to ground with a vertically mounted antenna) and aimed directly at the antenna's axis. These measurements are representative of persons other than the operator standing next to the vehicle.

Each of the offered antennas mounted at the center of the trunk were assessed at the rear of the vehicle while maintaining a twenty (20) centimeter separation distance between the probe sensor and vehicle body. The worst case antenna was then tested at a 45º radial at the corner of the trunk, and 90º radial at the side of the trunk.

For the current test vehicle, the antenna to probe sensor separation distance is 90cm (directly behind vehicle), 104 cm (45 degree radial) and 110.5 cm (90 degree radial).

Note: The distance from the trunk-mounted antenna to the edge of the vehicle is 42cm and the distance from the edge of the vehicle's trunk to the Survey Probe Sensor is 48cm.

5.1.2 Internal/Passenger vehicle EME measurement
(Antenna mounted at trunk center)

MPE measurements for passenger conditions are determined by taking the average of the (3) measurements (Head, Chest, and Lower Trunk) inside the vehicle for both the front and back seats. The measurement probe is positioned orthogonal to antenna (typically parallel to ground with a vertically mounted antenna), and aimed directly at the antenna's axis while the antenna is at 85cm from the back of the backseat passenger's head. These measurements are representative of operator and passengers sitting in the front and back seat of the vehicle.

5.2 EME measurements made with roof mounted antenna(s)
(Refer to APPENDIX A for antenna location and test distances)

5.2.1 External/Bystander vehicle EME measurement
(Antenna mounted at roof center)

MPE measurements for bystander conditions are determined by taking the average of (10) measurements in a 2m vertical line for the test location indicated in APPENDIX A with 20cm increments at the test distance of 90cm from the antenna under test. The measurement probe is positioned orthogonal to antenna (typically parallel to ground with a vertically mounted antenna) and aimed directly at the antenna's axis. These measurements are representative of persons other than the operator standing next to the vehicle.

Note: Actual test distance was approximately 117cm from antenna to probe element (97cm from antenna to edge of car door; 20cm vertical test line to car door); this is the closest distance that can be achieved to an antenna mounted to the center of the vehicle used for MPE compliance assessment.

5.2.2 Internal/Passenger vehicle EME measurement
(Antenna mounted at roof center)

MPE measurements for passenger conditions are determined by taking the average of the (3) measurements (Head, Chest, and Lower Trunk) inside the vehicle for both the front and back seats. The measurement probe is positioned orthogonal to antenna (typically parallel to ground with a vertically mounted antenna) and aimed directly at the antenna's axis. These measurements are representative of operator and passengers sitting in the front and back seat of the vehicle.

6.0 Test Site

The test site is the Motorola open area test site located at 8000 W. Sunrise Blvd., Plantation, FL. 33322.

7.0 Measurement System/Equipment

Equipment Type	Model #	SN	Calibration Date
Automobile	2003 Ford Crown Victoria, 4-Door		
Survey Meter	ETS Model HI-2200	00086316	1/31/2008; 5/23/2008
Probe: E-Field (Electric Field)	ETS Model E100	00084254	1/31/2008
Probe: H-Field (Magnetic Field)	ETS Model H200	00084183	5/23/2008

ETS equipments measured Power Density in mW/cm2.

8.0 DUT Output Power

Power density measurements were performed with the test frequencies and associated power levels presented in the table below.

Test Frequencies (MHz)	Measured Initial Power (W)
136.0125	120
147.4	120
149	120
155	120
160	118
173.9875	117

9.0 Test Set-Up Description

All antennas listed on the cover page of this report were considered in order to develop the test plan for this product.

a) The ¼ wave 2.15dBi gain antennas (HAD4006A, HAD4007A, HAD4008A, HAD4009A, HAD4016A, HAD4017A, HAD4021A), and the ½ wave 5.15dBi gain antenna (RAD4010ARB) were assessed while mounted at the center of the roof of the test vehicle.

b) The ½ wave 5.15dBi gain antenna (RAD4010ARB) was assessed while mounted at the center of the trunk of the test vehicle.

Assessments were performed with DUT (Device Under Test) installed on a test vehicle, while engine was at idle, at the specified distances and test locations indicated in sections 5.0, 10.0, and the APPENDIX A.

10.0 Test Results Summary

The tables below summarized the MPE measurement results for each test configuration: antenna (model and description), antenna gain, TX frequency, maximum output power, initial power, E/H field measurements, probe frequency cal factor, test positions (BS-Bystander, PB-Passenger Back, PF-Passenger Front), average over body results, calculated power density results, max calculated power density results, % of the applicable specification limit, and applicable IEEE/FCC specification limits.

MPE results for this mobile radio are based on 50% duty cycle which is in accordance with the User Manual instructions.

Below is an explanation of how the MPE results are calculated.

External to vehicle (Bystander) -10 measurements are averaged over the body (*body_avg*).
Internal to vehicle (Passengers) - 3 measurements are averaged over the body (*body_avg*).
The Average over Body test methodology is consistent with IEEE/ANSI C95.3-2002 guidelines.

Therefore;

$$Pwr\_density\_calc = body\_avg * (probe\_frequency\_cal\_factor)^2 * duty\_cycle$$

$$Pwr\_density\_\max\_calc = pwr\_density\_calc * \frac{\max\_output\_power}{initial\_output\_power}$$

Note1; For initial output power> max_output_power; max_output_power / initial output power = 1
Note2: The probe frequency cal factors used for MPE evaluation of this product are based on the worse case.
Note 3: The calibration certificate's frequency cal factors were determined by measuring V/m for E-field probe and A/m for H-field probe. The results presented herein are power density (mW/cm^2) and therefore the cal factors were squared as indicated in the formula above.

Table 1: E-field - MPE assessment data with antennas mounted on the roof

Ant. Model/ Desc.	Ant. Gain (dBi)	Tx Freq (MHz)	Max Pwr (W)	Initial Pwr (W)	Test Mode	E/H Field	Probe Freq. Cal Factor	Test Pos.	Avg. over Body (mW/ cm2)	Calc. (mW/ cm2)	Max Calc. (mW/ cm2)	% of Spec Limit	FCC Spec Limit (mW/ cm2)
HAD4021A (136 - 174 MHz, 1/4W)	2.15	136.0125	120	120	CW	E	1.02	BS	0.28	0.14	0.14	70	0.2
HAD4021A (136 - 174 MHz, 1/4W)	2.15	136.0125	120	120	CW	E	1.02	PB	0.31	0.16	0.16	80	0.2
HAD4021A (136 - 174 MHz, 1/4W)	2.15	136.0125	120	120	CW	E	1.02	PF	0.10	0.05	0.05	25	0.2
HAD4021A (136 - 174 MHz, 1/4W)	2.15	155	120	120	CW	E	1.04	BS	0.26	0.14	0.14	68	0.2
HAD4021A (136 - 174 MHz, 1/4W)	2.15	155	120	120	CW	E	1.04	PB	0.26	0.14	0.14	68	0.2
HAD4021A (136 - 174 MHz, 1/4W)	2.15	155	120	120	CW	E	1.04	PF	0.13	0.07	0.07	34	0.2
HAD4021A (136 - 174 MHz, 1/4W)	2.15	173.9875	120	117	CW	E	1.06	BS	0.25	0.13	0.13	67	0.2
HAD4021A (136 - 174 MHz, 1/4W)	2.15	173.9875	120	117	CW	E	1.06	PB	0.12	0.06	0.06	32	0.2
HAD4021A (136 - 174 MHz, 1/4W)	2.15	173.9875	120	117	CW	E	1.06	PF	0.05	0.03	0.03	14	0.2
HAD4006A (136-144 MHz, 1/4W)	2.15	136.0125	120	120	CW	E	1.02	BS	0.33	0.17	0.17	84	0.2
HAD4006A (136-144 MHz, 1/4W)	2.15	136.0125	120	120	CW	E	1.02	PB	0.36	0.19	0.19	93	0.2
HAD4006A (136-144 MHz, 1/4W)	2.15	136.0125	120	120	CW	E	1.02	PF	0.12	0.06	0.06	31	0.2
HAD4007A (144-150.8 MHz, 1/4W)	2.15	147.4	120	120	CW	E	1.03	BS	0.30	0.16	0.16	78	0.2
HAD4007A (144-150.8 MHz, 1/4W)	2.15	147.4	120	120	CW	E	1.03	PB	0.29	0.15	0.15	74	0.2
HAD4007A (144-150.8 MHz, 1/4W)	2.15	147.4	120	120	CW	E	1.03	PF	0.11	0.06	0.06	29	0.2

Table 1 (cont): E field - MPE assessment data with antenna mounted on the roof

Ant. Model/ Desc.	Ant. Gain (dBi)	Tx Freq (MHz)	Max Pwr (W)	Initial Pwr (W)	Test Mode	E/H Field	Probe Freq. Cal Factor	Test Pos.	Avg. over Body (mW/ cm2)	Calc. (mW/ cm2)	Max Calc. (mW/ cm2)	% of Spec Limit	FCC Spec Limit (mW/ cm2)
HAD4008A (150.8-162 MHz, 1/4W)	2.15	155	120	120	CW	E	1.04	BS	0.34	0.17	0.17	87	0.2
HAD4008A (150.8-162 MHz, 1/4W)	2.15	155	120	120	CW	E	1.04	PB	0.34	0.18	0.18	88	0.2
HAD4008A (150.8-162 MHz, 1/4W)	2.15	155	120	120	CW	E	1.04	PF	0.18	0.10	0.10	48	0.2
HAD4009A (162 - 174 MHz, 1/4W)	2.15	173.9875	120	117	CW	E	1.06	BS	0.34	0.18	0.18	92	0.2
HAD4009A (162 - 174 MHz, 1/4W)	2.15	173.9875	120	117	CW	E	1.06	PB	0.16	0.08	0.09	43	0.2
HAD4009A (162 - 174 MHz, 1/4W)	2.15	173.9875	120	117	CW	E	1.06	PF	0.07	0.04	0.04	20	0.2
HAD4016A (136 - 162 MHz, 1/4W)	2.15	136.0125	120	120	CW	E	1.02	BS	0.25	0.13	0.13	65	0.2
HAD4016A (136 - 162 MHz, 1/4W)	2.15	136.0125	120	120	CW	E	1.02	PB	0.32	0.16	0.16	81	0.2
HAD4016A (136 - 162 MHz, 1/4W)	2.15	136.0125	120	120	CW	E	1.02	PF	0.11	0.05	0.05	27	0.2
HAD4016A (136 - 162 MHz, 1/4W)	2.15	149	120	120	CW	E	1.03	BS	0.32	0.17	0.17	83	0.2
HAD4016A (136 - 162 MHz, 1/4W)	2.15	149	120	120	CW	E	1.03	PB	0.27	0.14	0.14	70	0.2
HAD4016A (136 - 162 MHz, 1/4W)	2.15	149	120	120	CW	E	1.03	PF	0.13	0.07	0.07	33	0.2
HAD4016A (136 - 162 MHz, 1/4W)	2.15	160	120	118	CW	E	1.04	BS	0.22	0.12	0.12	59	0.2
HAD4016A (136 - 162 MHz, 1/4W)	2.15	160	120	118	CW	E	1.04	PB	0.14	0.07	0.07	36	0.2
HAD4016A (136 - 162 MHz, 1/4W)	2.15	160	120	118	CW	E	1.04	PF	0.05	0.03	0.03	14	0.2

Table 1 (cont): E field - MPE assessment data with antenna mounted on the roof

Ant. Model/ Desc.	Ant. Gain (dBi)	Tx Freq (MHz)	Max Pwr (W)	Initial Pwr (W)	Test Mode	E/H Field	Probe Freq. Cal Factor	Test Pos.	Avg. over Body (mW/ cm2)	Calc. (mW/ cm2)	Max Calc. (mW/ cm2)	% of Spec Limit	FCC Spec Limit (mW/ cm2)
HAD4017A (146 - 174 MHz, 1/4W)	2.15	147.4	120	120	CW	E	1.03	BS	0.18	0.09	0.09	47	0.2
HAD4017A (146 - 174 MHz, 1/4W)	2.15	147.4	120	120	CW	E	1.03	PB	0.18	0.09	0.09	46	0.2
HAD4017A (146 - 174 MHz, 1/4W)	2.15	147.4	120	120	CW	E	1.03	PF	0.06	0.03	0.03	16	0.2
HAD4017A (146 - 174 MHz, 1/4W)	2.15	160	120	118	CW	E	1.04	BS	0.35	0.18	0.18	91	0.2
HAD4017A (146 - 174 MHz, 1/4W)	2.15	160	120	118	CW	E	1.04	PB	0.19	0.10	0.10	51	0.2
HAD4017A (146 - 174 MHz, 1/4W)	2.15	160	120	118	CW	E	1.04	PF	0.08	0.04	0.04	20	0.2
HAD4017A (146 - 174 MHz, 1/4W)	2.15	173.9875	120	117	CW	E	1.06	BS	0.28	0.15	0.15	76	0.2
HAD4017A (146 - 174 MHz, 1/4W)	2.15	173.9875	120	117	CW	E	1.06	PB	0.13	0.07	0.07	36	0.2
HAD4017A (146 - 174 MHz, 1/4W)	2.15	173.9875	120	117	CW	E	1.06	PF	0.07	0.04	0.04	18	0.2
RAD4010ARB (136 - 174 MHz, 1/2 Wave)	5.15	136.0125	120	120	CW	E	1.02	BS	0.16	0.08	0.08	40	0.2
RAD4010ARB (136 - 174 MHz, 1/2 Wave)	5.15	136.0125	120	120	CW	E	1.02	PB	0.08	0.04	0.04	20	0.2
RAD4010ARB (136 - 174 MHz, 1/2 Wave)	5.15	136.0125	120	120	CW	E	1.02	PF	0.01	0.01	0.01	3	0.2
RAD4010ARB (136 - 174 MHz, 1/2 Wave)	5.15	155	120	120	CW	E	1.04	BS	0.27	0.14	0.14	70	0.2
RAD4010ARB (136 - 174 MHz, 1/2 Wave)	5.15	155	120	120	CW	E	1.04	PB	0.09	0.05	0.05	24	0.2
RAD4010ARB (136 - 174 MHz, 1/2 Wave)	5.15	155	120	120	CW	E	1.04	PF	0.04	0.02	0.02	10	0.2
RAD4010ARB (136 - 174 MHz, 1/2 Wave)	5.15	173.9875	120	117	CW	E	1.06	BS	0.09	0.05	0.05	24	0.2
RAD4010ARB (136 - 174 MHz, 1/2 Wave)	5.15	173.9875	120	117	CW	E	1.06	PB	0.08	0.04	0.05	23	0.2
RAD4010ARB (136 - 174 MHz, 1/2 Wave)	5.15	173.9875	120	117	CW	E	1.06	PF	0.03	0.01	0.01	7	0.2

Table 2: H field - MPE assessment data with antenna mounted on the roof

Ant. Model/ Desc.	Ant. Gain (dBi)	Tx Freq (MHz)	Max Pwr (W)	Initial Pwr (W)	Test Mode	E/H Field	Probe Freq. Cal Factor	Test Pos.	Avg. over Body (mW/ cm2)	Calc. (mW/ cm2)	Max Calc. (mW/ cm2)	% of Spec Limit	FCC Spec Limit (mW/ cm2)
HAD4021A (136 - 174 MHz, 1/4W)	2.15	136.0125	120	120	CW	H	0.79	BS	0.33	0.13	0.13	65	0.2
HAD4021A (136 - 174 MHz, 1/4W)	2.15	136.0125	120	120	CW	H	0.79	PB	0.00	0.00	0.00	0	0.2
HAD4021A (136 - 174 MHz, 1/4W)	2.15	136.0125	120	120	CW	H	0.79	PF	0.00	0.00	0.00	0	0.2
HAD4021A (136 - 174 MHz, 1/4W)	2.15	155	120	120	CW	H	0.73	BS	0.14	0.05	0.05	26	0.2
HAD4021A (136 - 174 MHz, 1/4W)	2.15	155	120	120	CW	H	0.73	PB	0.00	0.00	0.00	0	0.2
HAD4021A (136 - 174 MHz, 1/4W)	2.15	155	120	120	CW	H	0.73	PF	0.00	0.00	0.00	0	0.2
HAD4021A (136 - 174 MHz, 1/4W)	2.15	173.9875	120	117	CW	H	0.70	BS	0.26	0.09	0.09	46	0.2
HAD4021A (136 - 174 MHz, 1/4W)	2.15	173.9875	120	117	CW	H	0.70	PB	0.00	0.00	0.00	0	0.2
HAD4021A (136 - 174 MHz, 1/4W)	2.15	173.9875	120	117	CW	H	0.70	PF	0.00	0.00	0.00	0	0.2
HAD4006A (136-144 MHz, 1/4W)	2.15	136.0125	120	120	CW	H	0.79	BS	0.43	0.17	0.17	84	0.2
HAD4006A (136-144 MHz, 1/4W)	2.15	136.0125	120	120	CW	H	0.79	PB	0.12	0.05	0.05	23	0.2
HAD4006A (136-144 MHz, 1/4W)	2.15	136.0125	120	120	CW	H	0.79	PF	0.00	0.00	0.00	0	0.2
HAD4007A (144-150.8 MHz, 1/4W)	2.15	147.4	120	120	CW	H	0.75	BS	0.31	0.12	0.12	58	0.2
HAD4007A (144-150.8 MHz, 1/4W)	2.15	147.4	120	120	CW	H	0.75	PB	0.15	0.06	0.06	29	0.2
HAD4007A (144-150.8 MHz, 1/4W)	2.15	147.4	120	120	CW	H	0.75	PF	0.00	0.00	0.00	0	0.2
HAD4008A (150.8-162 MHz, 1/4W)	2.15	155	120	120	CW	H	0.73	BS	0.28	0.10	0.10	52	0.2
HAD4008A (150.8-162 MHz, 1/4W)	2.15	155	120	120	CW	H	0.73	PB	0.14	0.05	0.05	25	0.2
HAD4008A (150.8-162 MHz, 1/4W)	2.15	155	120	120	CW	H	0.73	PF	0.00	0.00	0.00	0	0.2

Table 2 (cont): H field - MPE assessment data with antenna mounted on the roof

Ant. Model/ Desc.	Ant. Gain (dBi)	Tx Freq (MHz)	Max Pwr (W)	Initial Pwr (W)	Test Mode	E/H Field	Probe Freq. Cal Factor	Test Pos.	Avg. over Body (mW/ cm2)	Calc. (mW/ cm2)	Max Calc. (mW/ cm2)	% of Spec Limit	FCC Spec Limit (mW/ cm2)
HAD4009A (162 - 174 MHz, 1/4W)	2.15	173.9875	120	117	CW	H	0.70	BS	0.50	0.17	0.18	89	0.2
HAD4009A (162 - 174 MHz, 1/4W)	2.15	173.9875	120	117	CW	H	0.70	PB	0.00	0.00	0.00	0	0.2
HAD4009A (162 - 174 MHz, 1/4W)	2.15	173.9875	120	117	CW	H	0.70	PF	0.00	0.00	0.00	0	0.2
HAD4016A (136 - 162 MHz, 1/4W)	2.15	136.0125	120	120	CW	H	0.79	BS	0.32	0.13	0.13	63	0.2
HAD4016A (136 - 162 MHz, 1/4W)	2.15	136.0125	120	120	CW	H	0.79	PB	0.00	0.00	0.00	0	0.2
HAD4016A (136 - 162 MHz, 1/4W)	2.15	136.0125	120	120	CW	H	0.79	PF	0.00	0.00	0.00	0	0.2
HAD4016A (136 - 162 MHz, 1/4W)	2.15	149	120	120	CW	H	0.74	BS	0.37	0.14	0.14	68	0.2
HAD4016A (136 - 162 MHz, 1/4W)	2.15	149	120	120	CW	H	0.74	PB	0.15	0.06	0.06	28	0.2
HAD4016A (136 - 162 MHz, 1/4W)	2.15	149	120	120	CW	H	0.74	PF	0.00	0.00	0.00	0	0.2
HAD4016A (136 - 162 MHz, 1/4W)	2.15	160	120	118	CW	H	0.72	BS	0.21	0.07	0.08	38	0.2
HAD4016A (136 - 162 MHz, 1/4W)	2.15	160	120	118	CW	H	0.72	PB	0.00	0.00	0.00	0	0.2
HAD4016A (136 - 162 MHz, 1/4W)	2.15	160	120	118	CW	H	0.72	PF	0.00	0.00	0.00	0	0.2
HAD4017A (146 - 174 MHz, 1/4W)	2.15	147.4	120	120	CW	H	0.75	BS	0.11	0.04	0.04	20	0.2
HAD4017A (146 - 174 MHz, 1/4W)	2.15	147.4	120	120	CW	H	0.75	PB	0.00	0.00	0.00	0	0.2
HAD4017A (146 - 174 MHz, 1/4W)	2.15	147.4	120	120	CW	H	0.75	PF	0.00	0.00	0.00	0	0.2
HAD4017A (146 - 174 MHz, 1/4W)	2.15	160	120	118	CW	H	0.72	BS	0.31	0.11	0.11	56	0.2
HAD4017A (146 - 174 MHz, 1/4W)	2.15	160	120	118	CW	H	0.72	PB	0.00	0.00	0.00	0	0.2
HAD4017A (146 - 174 MHz, 1/4W)	2.15	160	120	118	CW	H	0.72	PF	0.00	0.00	0.00	0	0.2

Table 2 (cont): H field - MPE assessment data with antenna mounted on the roof

Ant. Model/ Desc.	Ant. Gain (dBi)	Tx Freq (MHz)	Max Pwr (W)	Initial Pwr (W)	Test Mode	E/H Field	Probe Freq. Cal Factor	Test Pos.	Avg. over Body (mW/ cm2)	Calc. (mW/ cm2)	Max Calc. (mW/ cm2)	% of Spec Limit	FCC Spec Limit (mW/ cm2)
HAD4017A (146 - 174 MHz, 1/4W)	2.15	173.9875	120	117	CW	H	0.70	BS	0.40	0.14	0.14	71	0.2
HAD4017A (146 - 174 MHz, 1/4W)	2.15	173.9875	120	117	CW	H	0.70	PB	0.00	0.00	0.00	0	0.2
HAD4017A (146 - 174 MHz, 1/4W)	2.15	173.9875	120	117	CW	H	0.70	PF	0.00	0.00	0.00	0	0.2
RAD4010ARB (136 - 174 MHz, 1/2 Wave)	5.15	136.0125	120	120	CW	H	0.79	BS	0.06	0.02	0.02	11	0.2
RAD4010ARB (136 - 174 MHz, 1/2 Wave)	5.15	136.0125	120	120	CW	H	0.79	PB	0.00	0.00	0.00	0	0.2
RAD4010ARB (136 - 174 MHz, 1/2 Wave)	5.15	136.0125	120	120	CW	H	0.79	PF	0.00	0.00	0.00	0	0.2
RAD4010ARB (136 - 174 MHz, 1/2 Wave)	5.15	155	120	120	CW	H	0.73	BS	0.23	0.09	0.09	43	0.2
RAD4010ARB (136 - 174 MHz, 1/2 Wave)	5.15	155	120	120	CW	H	0.73	PB	0.00	0.00	0.00	0	0.2
RAD4010ARB (136 - 174 MHz, 1/2 Wave)	5.15	155	120	120	CW	H	0.73	PF	0.00	0.00	0.00	0	0.2
RAD4010ARB (136 - 174 MHz, 1/2 Wave)	5.15	173.9875	120	117	CW	H	0.70	BS	0.35	0.12	0.13	63	0.2
RAD4010ARB (136 - 174 MHz, 1/2 Wave)	5.15	173.9875	120	117	CW	H	0.70	PB	0.00	0.00	0.00	0	0.2
RAD4010ARB (136 - 174 MHz, 1/2 Wave)	5.15	173.9875	120	117	CW	H	0.70	PF	0.00	0.00	0.00	0	0.2

Table 3: E field - MPE assessment data with antenna mounted on the trunk

Ant. Model/ Desc.	Ant. Gain (dBi)	Tx Freq (MHz)	Max Pwr (W)	Initial Pwr (W)	Test Mode	E/H Field	Probe Freq. Cal Factor	Test Pos.	Avg. over Body (mW/ cm2)	Calc. (mW/ cm2)	Max Calc. (mW/ cm2)	% of Spec Limit	FCC Spec Limit (mW/ cm2)
*RAD4010ARB (136 - 174 MHz, 1/2 Wave	5.15	136.0125	120	120	CW	E	1.02	BS	0.46	0.24	0.24	118	0.2
RAD4010ARB (136 - 174 MHz, 1/2 Wave)	5.15	136.0125	120	120	CW	E	1.02	PB	0.12	0.06	0.06	31	0.2
RAD4010ARB (136 - 174 MHz, 1/2 Wave)	5.15	136.0125	120	120	CW	E	1.02	PF	0.02	0.01	0.01	4	0.2
*RAD4010ARB (136 - 174 MHz, 1/2 Wave	5.15	155	120	120	CW	E	1.04	BS	0.64	0.33	0.33	166	0.2
RAD4010ARB (136 - 174 MHz, 1/2 Wave)	5.15	155	120	120	CW	E	1.04	PB	0.20	0.10	0.10	51	0.2
RAD4010ARB (136 - 174 MHz, 1/2 Wave)	5.15	155	120	120	CW	E	1.04	PF	0.03	0.01	0.01	7	0.2
*RAD4010ARB (136 - 174 MHz, 1/2 Wave	5.15	173.9875	120	117	CW	E	1.06	BS	0.83	0.44	0.45	226	0.2
*RAD4010ARB (136 - 174 MHz, 1/2 Wave	5.15	173.9875	120	117	CW	E	1.06	PB	0.90	0.48	0.49	246	0.2
RAD4010ARB (136 - 174 MHz, 1/2 Wave)	5.15	173.9875	120	117	CW	E	1.06	PF	0.18	0.10	0.10	49	0.2
---------- 45 Degree ---------													
*RAD4010ARB (136 - 174 MHz, 1/2 Wave	5.15	173.9875	120	117	CW	E	1.06	BS	0.62	0.33	0.34	169	0.2
---------- 90 Degree ----------													
*RAD4010ARB (136 - 174 MHz, 1/2 Wave	5.15	173.9875	120	117	CW	E	1.06	BS	0.57	0.30	0.31	154	0.2

* Test configuration exceeds MPE FCC spec limit

Table 4: H field - MPE assessment data with antenna mounted on the trunk

Ant. Model/ Desc.	Ant. Gain (dBi)	Tx Freq (MHz)	Max Pwr (W)	Initial Pwr (W)	Test Mode	E/H Field	Probe Freq. Cal Factor	Test Pos.	Avg. over Body (mW/ cm2)	Calc. (mW/ cm2)	Max Calc. (mW/ cm2)	% of Spec Limit	FCC Spec Limit (mW/ cm2)
*RAD4010ARB (136 - 174 MHz, 1/2 Wave	5.15	136.0125	120	120	CW	H	0.79	BS	0.62	0.24	0.24	122	0.2
RAD4010ARB (136 - 174 MHz, 1/2 Wave)	5.15	136.0125	120	120	CW	H	0.79	PB	0.00	0.00	0.00	0	0.2
RAD4010ARB (136 - 174 MHz, 1/2 Wave)	5.15	136.0125	120	120	CW	H	0.79	PF	0.00	0.00	0.00	0	0.2
*RAD4010ARB (136 - 174 MHz, 1/2 Wave	5.15	155	120	120	CW	H	0.73	BS	0.98	0.36	0.36	178	0.2
RAD4010ARB (136 - 174 MHz, 1/2 Wave)	5.15	155	120	120	CW	H	0.73	PB	0.00	0.00	0.00	0	0.2
RAD4010ARB (136 - 174 MHz, 1/2 Wave)	5.15	155	120	120	CW	H	0.73	PF	0.00	0.00	0.00	0	0.2
*RAD4010ARB (136 - 174 MHz, 1/2 Wave	5.15	173.9875	120	117	CW	H	0.70	BS	1.29	0.45	0.46	231	0.2
*RAD4010ARB (136 - 174 MHz, 1/2 Wave	5.15	173.9875	120	117	CW	H	0.70	PB	0.95	0.33	0.34	170	0.2
RAD4010ARB (136 - 174 MHz, 1/2 Wave)	5.15	173.9875	120	117	CW	H	0.70	PF	0.00	0.00	0.00	0	0.2
---------- 45 Degree ----------													
*RAD4010ARB (136 - 174 MHz, 1/2 Wave	5.15	173.9875	120	117	CW	H	0.70	BS	1.01	0.35	0.36	181	0.2
---------- 90 Degree ----------													
*RAD4010ARB (136 - 174 MHz, 1/2 Wave	5.15	173.9875	120	117	CW	H	0.7	BS	0.83	0.29	0.30	149	0.2

* Test configuration exceeds MPE FCC spec limit

11.0 Conclusion

The assessments for this device were performed with an output power range as indicated in section 8.0 The maximum allowable output power is equal to the upper limit of the final test factory transmit power specification of 120W for frequency range of 136 - 174MHz. The highest power density results for the mobile device scaled to the maximum allowable power output is 0.49mW/cm^2 for internal/passenger to the vehicle, and 0.46mW/cm^2 for external/bystander to the vehicle.

These MPE results demonstrate compliance to the FCC/IEEE Occupational/Controlled Exposure limit. FCC rules require compliance for passengers and bystanders to the FCC General Population/Uncontrolled limits. Although MPE is a convenient method of demonstrating compliance, SAR is recognized as the "basic restriction". For those configurations exceeding the MPE limit noted in section 11.0 table, compliance to the FCC SAR General Population/Uncontrolled limit of 1.6mW/g is demonstrated in Appendix E via SAR computational analysis.

The computation results show that this device, when used with the specified antennas, exhibit a maximum peak 1-g average SAR of 0.813 mW/g.

APPENDIX A
Illustration of Antenna Locations and Test Distances

Antenna Location Drawing with Test Locations Identified

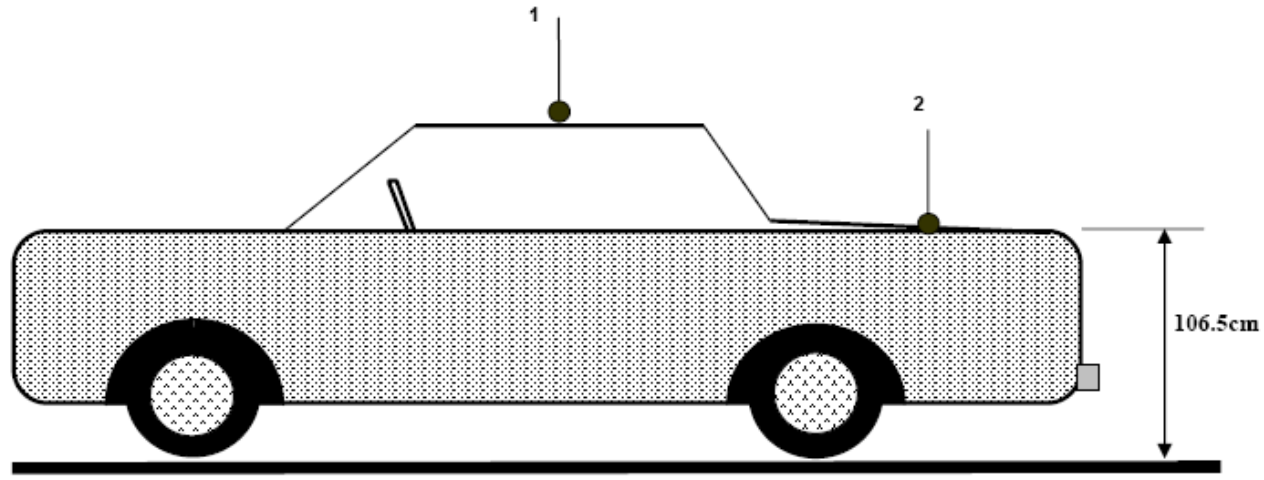

1 - Roof (center)
2 - Trunk (center)

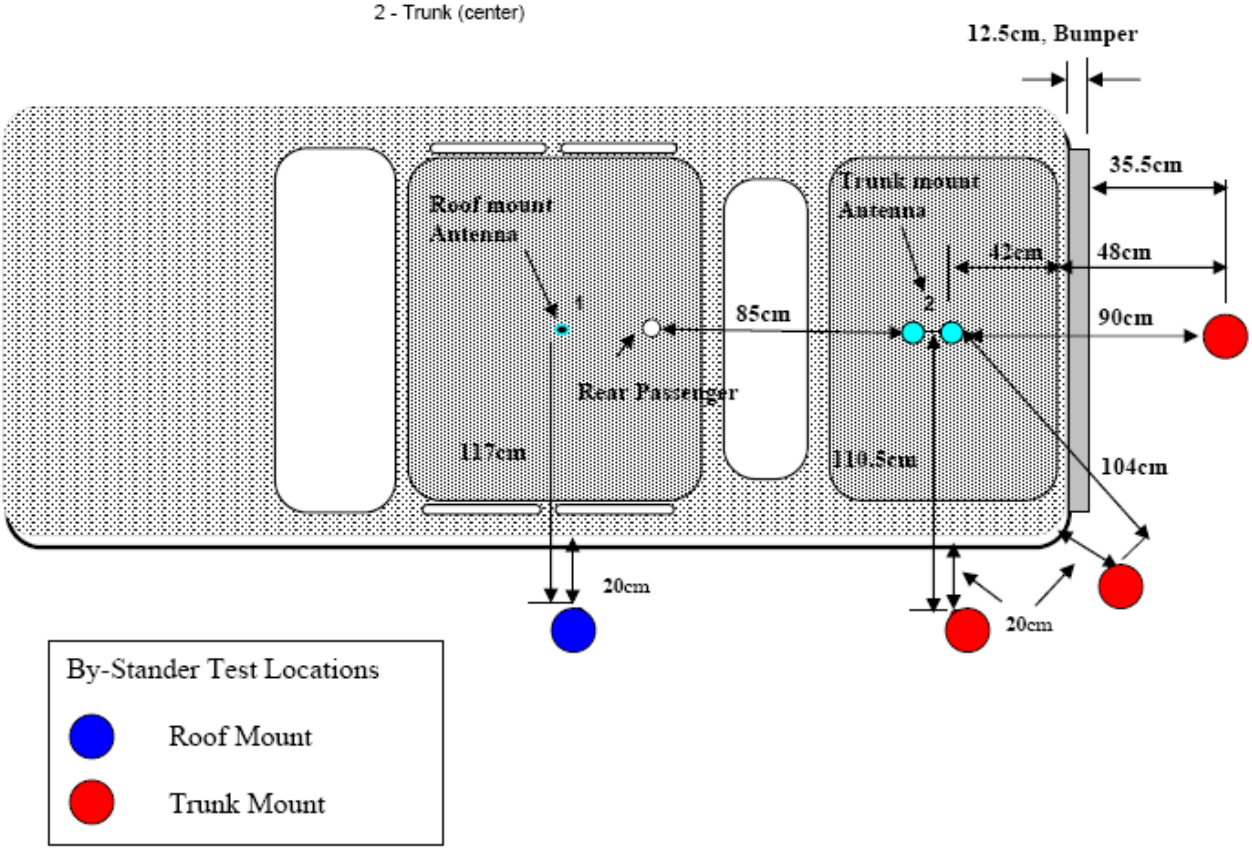

APPENDIX B
Meter/Probe Calibration Certificates

ACCREDITED

ETS-LINDGREN
An ESCO Technologies Company
1301 Arrow Point Drive
Cedar Park, Texas 78613
(512) 531-6498

ETS-LINDGREN
An ESCO Technologies Company
Track# J126811 Ltd Cal ☐
By MR Date 31-Jan-08
Next Cal Due
www.ets-lindgren.com

Cert I.D.: 67395
Lab Code 115844/1207.01

Certificate of Calibration Conformance

Page 1 of 4

The instrument identified below has been individually calibrated in compliance with the following standard(s):

IEEE 1309 - 2005, Institute of Electrical and Electronics Engineers, Standard for Calibration of Electromagnetic Field Sensors and Probes, Excluding Antennas from 9 kHz to 40 GHz

Environment: Laboratory MTE is maintained in a temperature controlled environment with ambient conditions from 18 to 28 C, relative humidity less than 90%. The instrument under test has been calibrated in a suitable environment using an EMCO TEM Cell 5101C, GTEM! 5305 and an RF Shielded EMC Chamber which is conducive to maintaining accurate and reliable measurement quality.

Manufacturer:	ETS-Lindgren	**Operating Range:**	100kHz - 5GHz
Model Number:	E100	**Instrument Type:**	Isotropic Probe > 1 GHz
Serial Number / ID:	**00084254**		
Tracking Number:	*J126811*		
Date Completed:	31-Jan-08		
Test Type:	Standard Field, Field Strength		
Calibration Uncertainty: k=2, (95% Confidence Level)	Std Field Method	10kHz - 18000 MHz, +/-0.7 dB, 26.5GHz - 40GHz, +/- 0.95 dB	

Test Remarks: Special Cal: A2LA Calibration. This certificate supercedes certificate with cert identification number 65434 and notes that the E100 was calibrated with metering unit model HI-2200, S/N 00086316.

Calibration Traceability: All Measuring and Test Equipment (M/TE) identified below are traceable to the National Institute for Standards and Technology (NIST). Calibration Laboratory and Quality System controls are compliant with ISO/IEC 17025-2005.

Standards and Equipment Used:
Make / Model / Name / S/N / Recall Date

Boonton	9200B	RF Voltmeter	324501AE	20-May-09
Hewlett Packard	437B	HP Power Meter	3125U12370	21-May-09
Fluke	6060B	RF Signal Generator	5690204	20-May-09
Marconi	2022	Signal Generator	119019/077	01-Nov-08
Rohde & Schwarz	857.8008.0	Power Meter NRVD	828110/019	24-Oct-08
Hewlett Packard	8648C	Signal Generator	3836A04299	29-Oct-08
Hewlett Packard	E4419B	HP Power Meter	US39250717	29-Oct-08
Hewlett Packard	83650L	Synthesized Sweep Gen	3844A00422	07-Aug-08

Condition of Instrument On Release:
In Tolerance to Internal Quality Standards

Maynard M Reich

Calibration Completed By
Maynard Reich, Calibration Technician

Attested and Issued on 31-Jan-08
Ronald W. Bethel, Calibration Manager

ETS·LINDGREN™

An ESCO Technologies Company

Frequency Response Calibration Factors
Model E100 Serial Number 00084254
Model HI-2200 Serial Number 00086316
Date of Calibration 30 Jan 2008

Frequency	Applied	Probe Reading			Correction Factor			
(MHz)	V/m	X	Y	Z	X	Y	Z	Avg
0.10	8.03	4.12	4.15	4.47	1.95	1.93	1.80	1.89
0.10	19.94	10.29	10.47	11.34	1.94	1.91	1.76	1.87
0.10	70.04	35.88	36.53	39.78	1.95	1.92	1.76	1.88
0.10	124.74	65.46	66.55	71.88	1.90	1.87	1.74	1.84
0.50	8.02	6.23	6.03	6.05	1.29	1.33	1.33	1.31
0.50	20.06	15.69	15.20	15.19	1.28	1.32	1.32	1.31
0.50	70.13	55.13	53.28	53.22	1.27	1.32	1.32	1.30
0.50	124.69	95.63	92.77	92.71	1.30	1.34	1.35	1.33
1.00	7.97	6.77	6.80	6.72	1.18	1.17	1.19	1.18
1.00	20.05	17.17	17.21	16.91	1.17	1.16	1.19	1.17
1.00	69.79	60.03	60.21	59.10	1.16	1.16	1.18	1.17
1.00	125.44	105.58	105.77	103.91	1.19	1.19	1.21	1.19
10.00	7.99	7.87	7.95	7.83	1.02	1.00	1.02	1.01
10.00	19.96	19.52	19.69	19.37	1.02	1.01	1.03	1.02
10.00	70.08	69.68	70.27	68.29	1.01	1.00	1.02	1.01
10.00	124.98	121.19	122.31	120.25	1.03	1.02	1.04	1.03
20.00	7.98	8.20	8.36	8.16	0.97	0.96	0.97	0.97
20.00	20.02	20.40	20.62	20.26	0.98	0.97	0.99	0.98
20.00	70.13	72.57	73.09	71.22	0.97	0.96	0.98	0.97
20.00	125.00	125.87	126.85	125.07	0.99	0.99	1.00	0.99
50.00	8.00	8.18	8.23	8.14	0.98	0.97	0.98	0.98
50.00	20.00	20.34	20.51	20.23	0.98	0.98	0.99	0.98
50.00	70.01	71.96	72.41	71.55	0.97	0.97	0.98	0.97
50.00	124.45	125.65	126.38	124.99	0.99	0.99	1.00	0.99
100.00	8.02	8.27	8.33	8.22	0.97	0.96	0.98	0.97
100.00	19.95	20.35	20.47	20.20	0.98	0.97	0.99	0.98
100.00	69.85	72.08	72.54	71.59	0.97	0.96	0.98	0.97
100.00	124.68	126.15	126.88	125.44	0.99	0.98	0.99	0.99
200.00	7.96	7.68	7.73	7.61	1.04	1.03	1.05	1.04
200.00	20.05	19.41	19.56	19.20	1.03	1.02	1.05	1.03
200.00	70.15	71.38	71.82	70.46	0.98	0.98	1.00	0.99
200.00	125.61	126.61	127.52	125.04	0.99	0.99	1.00	0.99
300.00	8.01	8.16	8.20	8.12	0.98	0.98	0.99	0.98
300.00	19.96	20.38	20.58	20.30	0.98	0.97	0.98	0.98
300.00	69.88	74.06	74.59	73.72	0.94	0.94	0.95	0.94
300.00	125.02	129.94	130.46	129.20	0.96	0.96	0.97	0.96
400.00	8.01	8.16	8.21	8.12	0.98	0.98	0.99	0.98
400.00	20.07	20.22	20.36	20.09	0.99	0.99	1.00	0.99
400.00	70.23	72.01	72.56	71.69	0.98	0.97	0.98	0.97
400.00	125.18	125.78	126.61	124.89	1.00	0.99	1.00	1.00
500.00	8.01	7.98	8.04	7.93	1.00	1.00	1.01	1.00
500.00	20.02	19.77	19.78	19.64	1.01	1.01	1.02	1.01
500.00	69.94	70.70	71.21	70.05	0.99	0.98	1.00	0.99
500.00	125.54	124.25	125.23	123.16	1.01	1.00	1.02	1.01
600.00	7.99	7.71	7.80	7.81	1.03	1.02	1.03	1.03
600.00	19.99	19.21	19.37	19.13	1.04	1.03	1.04	1.04
600.00	70.10	68.54	69.74	68.96	1.02	1.01	1.02	1.01
600.00	124.57	120.13	120.81	119.24	1.04	1.03	1.04	1.04

ETS·LINDGREN™

Frequency Response Calibration Factors
Model E100 Serial Number 00084254
Model HI-2200 Serial Number 00086316
Date of Calibration 30 Jan 2008

Frequency	Applied	Probe Reading			Correction Factor			
(MHz)	V/m	X	Y	Z	X	Y	Z	Avg
700.00	8.00	7.62	7.66	7.62	1.05	1.04	1.05	1.05
700.00	20.09	18.95	19.09	18.88	1.06	1.05	1.06	1.06
700.00	70.17	67.73	68.03	67.46	1.04	1.03	1.04	1.04
700.00	125.71	118.37	119.17	118.02	1.06	1.05	1.06	1.06
800.00	7.97	7.35	7.40	7.33	1.08	1.08	1.09	1.08
800.00	20.05	18.18	18.55	18.24	1.10	1.08	1.10	1.09
800.00	69.92	65.21	66.16	64.55	1.07	1.06	1.08	1.07
800.00	125.05	113.91	114.81	112.95	1.10	1.09	1.11	1.10
900.00	7.99	7.96	8.05	7.91	1.00	0.99	1.01	1.00
900.00	20.00	19.67	19.89	19.51	1.02	1.01	1.03	1.02
900.00	70.25	70.29	70.89	69.50	1.00	0.99	1.01	1.00
900.00	125.12	122.01	123.30	120.78	1.03	1.01	1.04	1.03
1000.00	8.04	8.16	8.23	8.15	0.98	0.98	0.99	0.98
1000.00	20.08	20.12	20.25	20.04	1.00	0.99	1.00	1.00
1000.00	69.74	70.56	70.96	70.26	0.99	0.98	0.99	0.99
1000.00	124.61	122.72	123.56	122.22	1.02	1.01	1.02	1.01
2000.00	20.00	20.00	19.97	19.60	1.00	1.00	1.02	1.01
3000.00	20.10	19.70	20.18	18.99	1.02	1.00	1.06	1.02
4000.00	19.97	20.05	19.91	19.23	1.00	1.00	1.04	1.01
5000.00	19.74	15.47	15.42	14.57	1.28	1.28	1.36	1.30
6000.00	20.05	14.08	14.97	14.95	1.42	1.34	1.34	1.37

ETS·LINDGREN™
An ESCO Technologies Company

PROBE ROTATIONAL RESPONSE

Model	E100
S/N	00084254
Date	31-Jan-2008
Time	09:53:13
Variation	0.30 dB

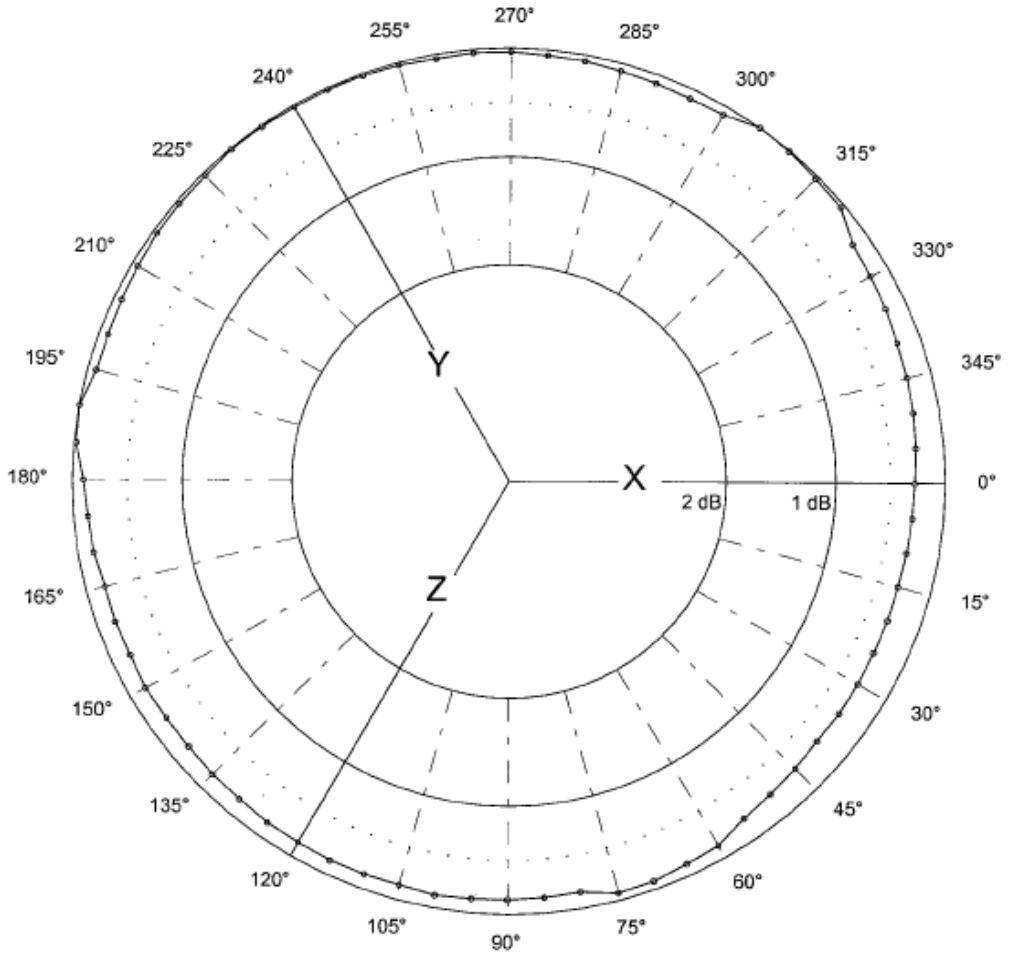

- Isotropic response measured in a 20 V/m field at 400 MHz

Page 4 of 4

ETS·LINDGREN™

An ESCO Technologies Company

CALIBRATION REPORT

Magnetic Field Sensor

Model	*S/N*
H200	00084183
HI-2200	00086316

As received, the instrument was found: X Within Tolerance
_____ Out of Tolerance
_____ (New Instrument)

Frequency Response

Frequency Response		*Nominal Field*	*Cal Factor**	*Deviation*
	MHz	*A/m*	(Applied/Indicated)	*dB*
1	5	0.08	1.23	-1.81
2	10	0.08	1.05	-0.46
3	15	0.08	1.02	-0.18
4	30	0.08	0.98	0.15
5	50	0.08	0.95	0.42
6	75	0.08	0.98	0.20
7	100	0.08	0.95	0.48
8	150	0.08	0.86	1.29
9	200	0.08	0.81	1.81
10	250	0.08	0.68	3.39
11	300	0.08	0.58	4.74

* Corrected magnetic field values (A/m) can be obtained by multiplying the Cal Factor with the indicated H field readings.

Linearity

Maximum linearity deviation is 0.03 dB

(measurements taken from 30 mA/m to 9 A/m at 27.12 MHz)

Test Conditions

Calibration performed at ambient room temperature: 23 ±3°C

The above sensor was calibrated to factory specifications. This calibration is performed per IEEE 1309 standard. All equipment used are traceable to US National Institute of Standards and Technology (NIST).

By: Maynard Rivera

Calibration Date: 23-May-2008

CALIBRATION
BY
DUE 513364

1301 Arrow Point Drive • Cedar Park, Texas 78613 • Phone 512.531.6400 • Fax 512.531.6500
info@ets-lindgren.com • www.ets-lindgren.com

APPENDIX C
DUT Photos
(Refer to Exhibit 7B)

APPENDIX D
SAR Simulation Report

MOTOROLA LABS

COMPUTATIONAL EME COMPLIANCE ASSESSMENT OF THE VHF MOBILE RADIO, MODEL # M30KTS9PW1AN, FCC ID AZ492FT3821

June 17, 2008

Giorgi Bit-Babik, Ph.D., and Antonio Faraone, Ph.D.
Motorola Corporate EME Research Lab, Plantation, Florida

Introduction

This report summarizes the computational [numerical modeling] analysis performed to document compliance of the VHF, Model Number M30KTS9PW1AN, Mobile Radio and vehicle-mounted antennas with the Federal Communications Commission (FCC) guidelines for human exposure to radio frequency (RF) emissions. The radio operates in the 136 - 174 MHz frequency band.

This computational analysis supplements the measurements conducted to evaluate the FCC *maximum permissible exposure* (MPE) limits for this mobile device. All test conditions (6 in total) that did not conform with applicable MPE limits were analyzed to determine whether those conditions complied with the *specific absorption rate* (SAR) limits for general public exposure (1.6 W/kg averaged over 1 gram of tissue and 0.08 W/kg averaged over the whole body) set forth in FCC guidelines, which are based on the IEEE C95.1-1999 standard [1]. In total 12 independent simulations have been performed. Ten simulations are addressing exposure of bystander and another two simulations are addressing exposure of passenger to the VHF mobile radios with trunk-mount antennas. For all simulations a commercial code based on Finite-Difference-Time-Domain (FDTD) methodology was employed to carry out the computational analysis. It is well established and recognized within the scientific community that SAR is the primary dosimetric quantity used to evaluate the human body's absorption of RF energy and that MPEs are

in fact derived from SAR. Accordingly, the SAR computations provide a scientifically valid and more relevant estimate of human exposure to RF energy.

Method

The simulation code employed is XFDTD™ v6.4, by Remcom Inc., State College, PA. This computational suite features a heterogeneous full body standing model (High Fidelity Body Mesh), derived from the so-called Visible Human [2], discretized in 5 mm voxels. The dielectric properties of 23 body tissues are automatically assigned by XFDTD™ at any specific frequency. The "seated" man model was obtained from the standing model by modifying the articulation angles at the hips and the knees. Details of the computational method and model are provided in the Appendix to this report, following the structure outlined in Appendix B.III of the Supplement C to the FCC OET Bulletin 65.

The car model has been imported into XFDTD™ from the CAD file of a sedan car having dimensions 4.98 m (L) x 1.85 m (W) x 1.18 m (H), and discretized in 5mm voxels. For the car model the wheels and part of the hood were omitted in order to fit within the computational memory available. These omissions would not be expected to affect the exposure calculations in any event.

For bystander exposure, the antenna position is 26 cm from the end of the trunk, so as to replicate the experimental conditions used in MPE measurements. For passenger exposure, the distance of trunk mounted antennas from the passenger head was set at 85 cm, so as to replicate the experimental conditions used in MPE measurements. Figures 1 and 2 show one of the XFDTD™ computational models used for bystander exposure. According to the latest IEEE 1528.2 draft standard (February 19, 2007) for bystander exposure simulations from vehicle mount antennas the lossy dielectric slab with 30 cm thickness, dielectric constant of 8 and conductivity of 0.01 S/m has been introduced in the computational model to properly account for the effect of the ground (pavement) on exposure. Figure 3 shows some of the XFDTD™ computational models used for passenger exposure to trunk mounted antennas.

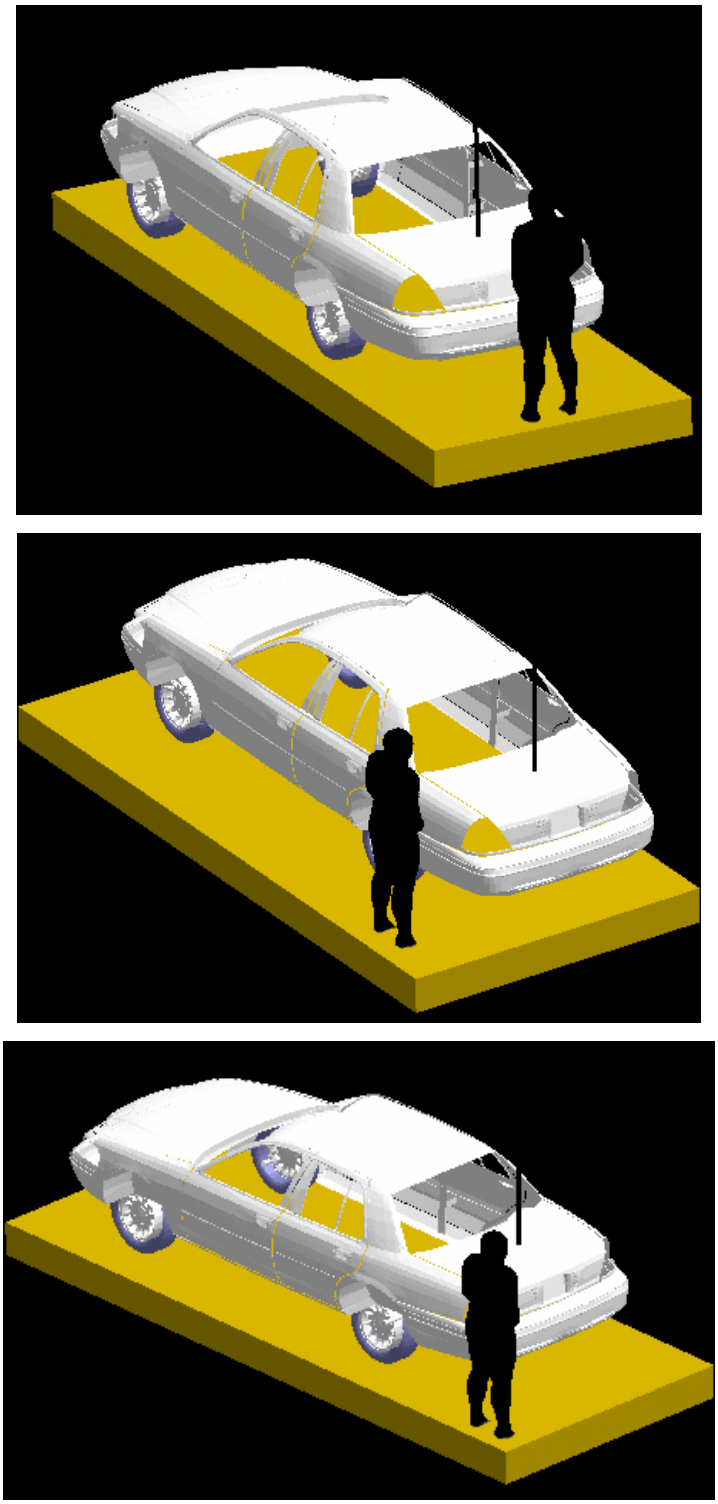

Figure 1: Bystander model exposed to a trunk-mount VHF antenna: Bystander is located at the back, on the side or at the corner of the car replicating the measurement conditions. The antenna is mounted in the center of the trunk. The dielectric slab under the car is introduced to model the ground (pavement) effect on exposure.

Figure 2: Top view of bystander exposure model four different locations relative to the vehicle model that replicate the measurement conditions.

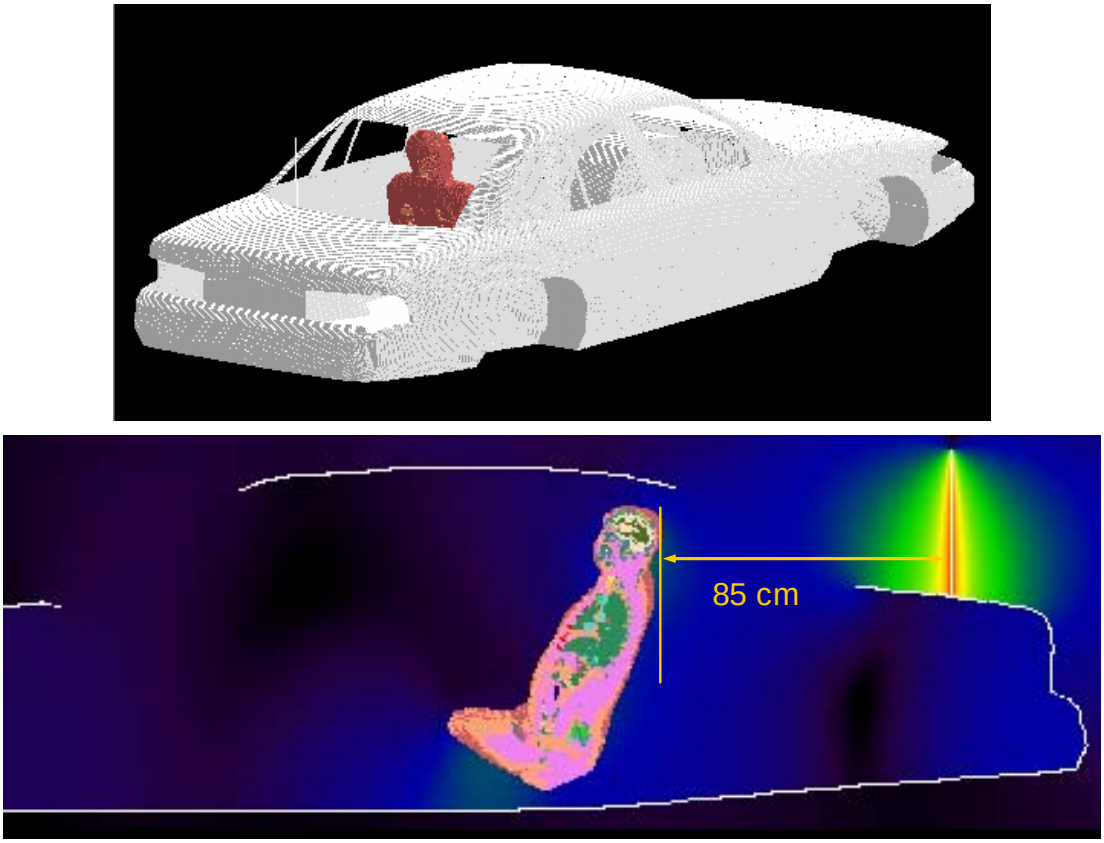

Figure 3: Passenger model exposed to a trunk-mount antenna operating: XFDTD geometry and H-field distribution. The antenna is mounted at 85 cm from the passenger.

The computational code employs a time-harmonic excitation to produce a steady state electromagnetic field in the exposed body. Subsequently, the corresponding SAR distribution is automatically processed in order to determine the whole-body and 1-g average SAR. The maximum output power from mobile radio antenna is 120 W *rms*. Since the ohmic losses in the cable and in the car materials, as well as the mismatch losses at the antenna feed-point, are neglected, and source-based time averaging (50% talk time) is employed, all computational results are normalized to half of it, i.e., 60 W *rms* net output power.

Results of SAR computations for car passengers

The test condition requiring SAR computations is summarized in Table I, together with the antenna data and the SAR results. The condition is for antenna mounted on the trunk. The passenger is located in the center or on the side of the rear seat. The passenger model is surrounded by air, as the seat, which is made out of poorly conductive fabrics, is not included in the computational model. All the transmit frequency, antenna length, and passenger location combinations reported in Table I have been simulated individually.

Table I: Results of the SAR computations for passenger exposure (50% talk-time).

Mount location	Antenna Kit #	Antenna length		Freq [MHz]	Exposure location	SAR [W/kg]	
		Physical	XFDTD			1-g	WB
Trunk	RAD4010ARB	103.5 cm	103.5 cm	174	center	0.221	0.0089
Trunk	RAD4010ARB	103.5 cm	103.5 cm	174	Side	0.228	0.0084

The SAR distribution in the passenger model in the exposure condition that gave highest 1-g SAR is reported in Figure 4 (174 MHz, passenger on the side of the back seat, RAD4010ARB antenna).

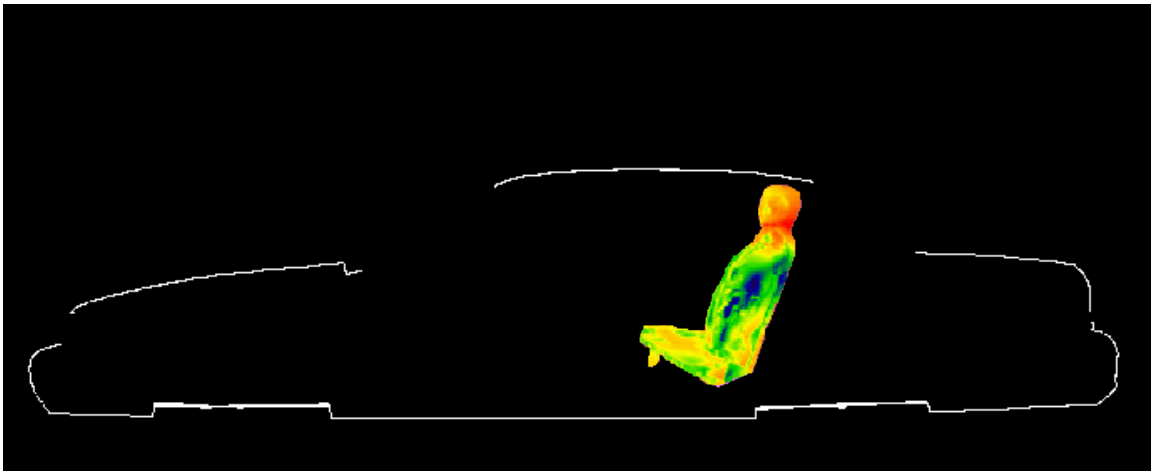

Figure 4. SAR distribution at 174 MHz in the passenger located on the side of the back seat, produced by the trunk-mount RAD4010ARB antenna (103.5 cm). The contour plot in the figure is relative to the plane where the peak 1-g average SAR for this exposure condition occurs.

The two pictures below in Figure 5 show the E and H field distributions in the plane of the antenna corresponding to the condition in Figure 4.

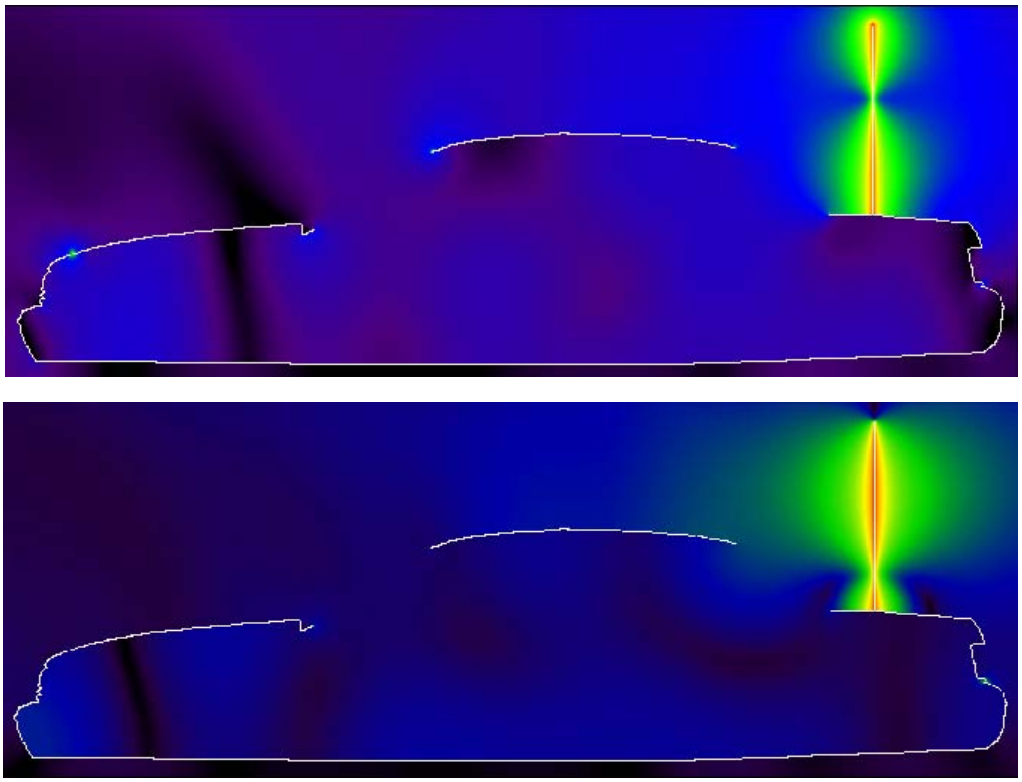

a)

b)

Figure 5. (a) E-field distribution corresponding to exposure condition of Figure 4, and (b) H-field distribution corresponding to exposure condition of Figure 4.

Results of SAR computations for bystanders

The test conditions requiring SAR computations are summarized in Table II, together with other relevant information and the SAR results. With trunk mount antennas, the bystander is placed at the corner of the trunk, at the back of the trunk or on the side of the trunk at a distance of 90 cm from the antenna while maintaining at least 20 cm from the vehicle body, so as to replicate the conditions used in MPE measurements. Two cases of bystander - facing towards or away from the car - were simulated individually.

Table II: Results of the SAR computations for bystander exposure (50% talk-time) at a separation distance of 90 cm from the trunk-mount antenna while maintaining at least 20 cm from the vehicle body.

Mount location	Antenna Kit #	Antenna length		Freq [MHz]	Exposure location	SAR [W/kg]	
		Physical	XFDTD			1-g	WB
Trunk	RAD4010ARB	143.5 cm	143.5 cm	136	Back	0.218	0.0087
Trunk	RAD4010ARB	121.5 cm	121.5 cm	155	Back	0.373	0.0132
Trunk	RAD4010ARB	103.5 cm	103.5 cm	174	Back	0.684	0.0231
Trunk, 45 deg	RAD4010ARB	103.5 cm	103.5 cm	174	Back	0.327	0.0151
Trunk, 90 deg	RAD4010ARB	103.5 cm	103.5 cm	174	Back	0.371	0.0164
Trunk	RAD4010ARB	143.5 cm	143.5 cm	136	Front	0.300	0.0092
Trunk	RAD4010ARB	121.5 cm	121.5 cm	155	Front	0.502	0.0153
Trunk	RAD4010ARB	103.5 cm	103.5 cm	174	Front	0.813	0.0248
Trunk, 45 deg	RAD4010ARB	103.5 cm	103.5 cm	174	Front	0.367	0.0163
Trunk, 90 deg	RAD4010ARB	103.5 cm	103.5 cm	174	Front	0.496	0.0156

The SAR distribution in the bystander model in the exposure condition that gave highest 1-g SAR is reported in Figure 7 (174 MHz, bystander at the back of the trunk facing the car, RAD4010ARB antenna). The same condition produced highest whole body average SAR.

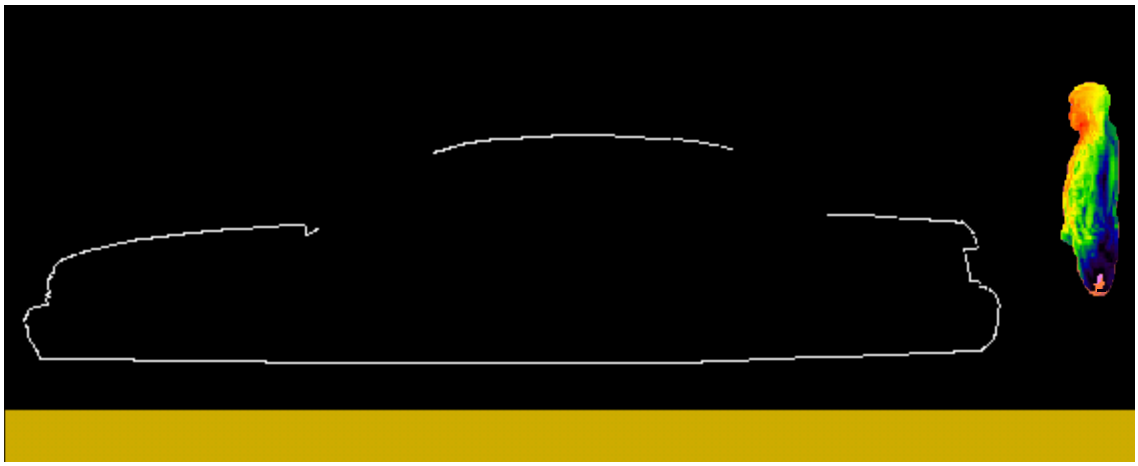

Figure 7. SAR distribution at 174 MHz in the bystander located at back the trunk, produced by the trunk-mount RAD4010ARB antenna. The contour plot for SAR distribution in the figure is relative to the plane where the peak 1-g average SAR for this exposure condition occurs.

The two pictures below show the E and H field distributions in the plane of the antenna corresponding to the condition represented in Figure 7.

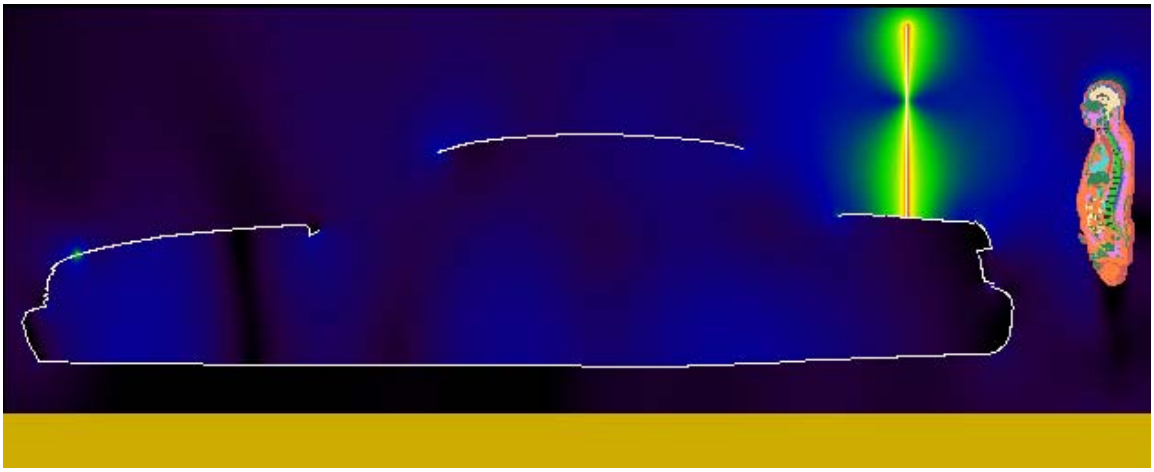

a)

b)

Figure 8. (a) E-field distribution in the plane of the antenna corresponding to exposure condition of Figure 7, and (b) H-field distribution corresponding to exposure condition of Figure 7.

Another example of the E and H field distributions of the gain trunk mounted antenna (RAD4010ARB) in the condition of bystander exposure at 174 MHz is shown in Figure 9

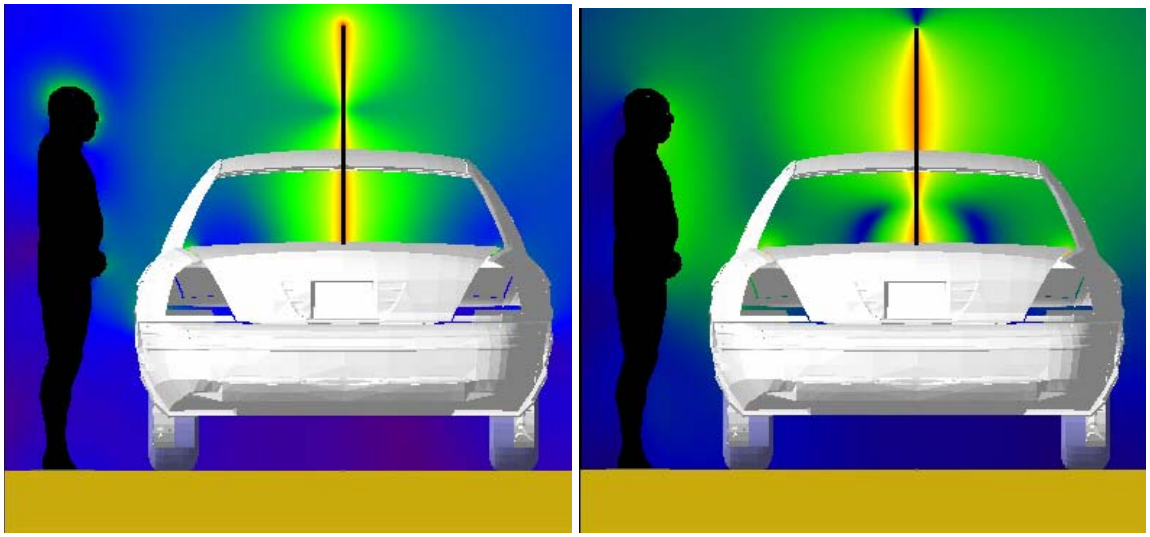

a) b)

Figure 9. (a) E-field distribution and (b) H-field distribution in the plane of the antenna corresponding to the bystander exposure condition located on the side of the trunk (RAD4010ARB antenna at 174 MHz)

The overall maximum peak 1-g SAR in all simulated conditions is 0.813 W/kg, less than the 1.6 W/kg limit, while the maximum whole-body average SAR is 0.0248 W/kg, less than the 0.08 W/kg limit.

Conclusions

Under the test conditions described for evaluating passenger and bystander exposure to the RF electromagnetic fields emitted by vehicle-mounted antennas used in conjunction with this mobile radio product, the present analysis shows that the computed SAR values are compliant with the FCC exposure limits for the general public.

References

[1] IEEE Standard C95.1-1999. *IEEE Standard for Safety Levels with Respect to Human Exposure to RF Electromagnetic Fields*, 3 kHz to 300 GHz.

[2] http://www.nlm.nih.gov/research/visible/visible_human.html

APPENDIX: SPECIFIC INFORMATION FOR SAR COMPUTATIONS

This appendix follows the structure outlined in Appendix B.III of the Supplement C to the FCC OET Bulletin 65. Most of the information regarding the code employed to perform the numerical computations has been adapted from the draft IEEE 1528.1 and 1528.2 standards, and from the XFDTD™ v5.3 and v6.4. User Manuals. Remcom Inc., owner of XFDTD™, is kindly acknowledged for the help provided.

1) Computational resources

a) A distributed Linux based multi-CPU computer cluster equipped with AMD 64-bit Opteron processors was employed for all simulations.

b) The memory requirement was close to 3 GB in all cases. Using the above-mentioned system with four processors operating concurrently, the typical simulation would run for 3 hours.

2) FDTD algorithm implementation and validation

a) We employed a commercial code (XFDTD™ v6.4, by Remcom Inc.) that implements the Yee's FDTD formulation [1]. The solution domain was discretized according to a rectangular grid with a uniform 5 mm step in all directions. Sub-gridding was not used. Liao's absorbing boundary conditions [2] are set at the domain boundary to simulate free space radiation processes. The excitation is a lumped voltage generator with 50-ohm source impedance. The code allows selecting *wire objects* without specifying their radius. We used a wire to represent the antenna. The car body is modeled by solid metal. We did not employ the "thin wire" algorithm in XFDTD™ since the antenna radius was never smaller than one-fifth the voxel dimension. In fact, the XFDTD™ manual specifies that "Thin Wire materials may be used in special situations where a wire with a radius much smaller than the cell size is required… in cases where the wire radius is important to the calculation and is less than approximately 1/5 the cell size, the thin wire material may be used to accurately simulate the correct wire dimensions." The voxel size in all our simulations was 5 mm, and the antenna radius is always at least 1 mm (1 mm for the short quarter-wave antennas and 1.5 mm for the long gain antennas), so there was no need to specify a "thin wire" material. Because the field impinges on the bystander or passenger model at a distance of several tens of voxels from the antenna, the details of antenna wire modeling are not expected to have significant impact on the exposure level.

b) XFDTD™ is one of the most widely employed commercial codes for electromagnetic simulations. It has gone through extensive validation and has proven its accuracy over time in many different applications. One example is provided in [3].

We carried out a validation of the code algorithm by running the canonical test case involving a half-wave wire dipole. The dipole is 0.475 times the free space wavelength at 160 MHz, i.e., 88.5 cm long. The discretization used in the model was uniform in all directions and equal to 5 mm, so the dipole was 177 cells long. Also in this case, the "thin

wire" model was not needed. The following picture shows XFDTD™ outputs regarding the antenna feed-point impedance (72.6 – j 11.6 ohm), as well as qualitative distributions of the total E and H fields near the dipole. The radiation pattern is shown as well (one lobe in elevation). As expected, the 3 dB beamwidth is about 78 degrees.

Total E-field **Total H-field**

Complex Feed Point Impedance (Ohms)

Feed	Real	Imaginary
1	72.553001	-11.623300

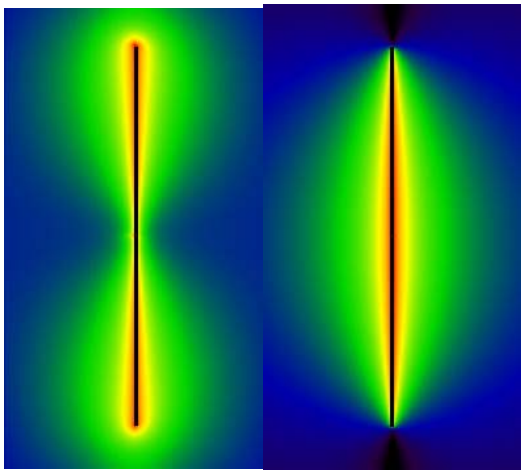

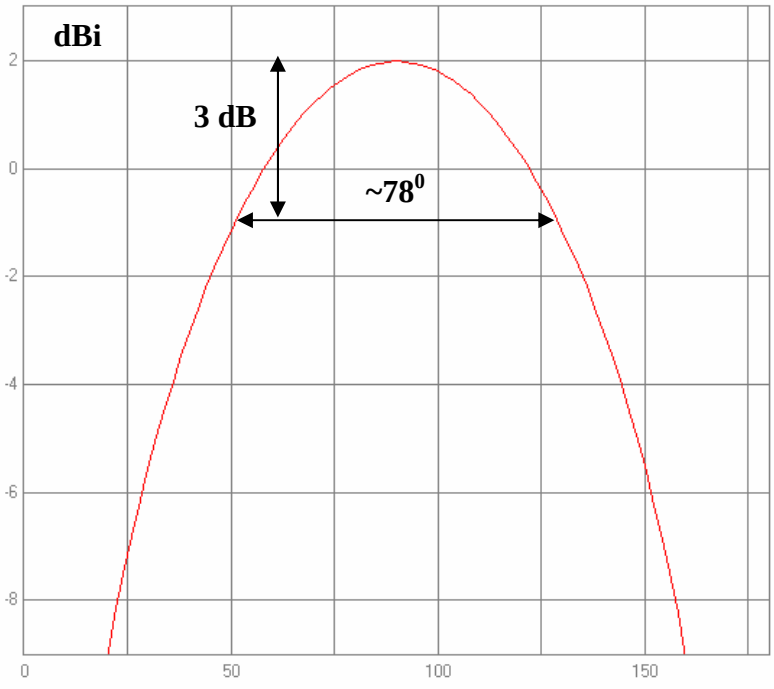

Elevation Angle [degrees]

We also compared the XFDTD™ result with the results derived from NEC [4], which is a code based on the method of moments. In this case, we used a dipole with radius 1

mm, length 88.5 cm, and the discretization is 5 mm. The corresponding input impedance at 160 MHz is 69.5-j10.5 ohm. Its frequency dependence is reported in the following figure.

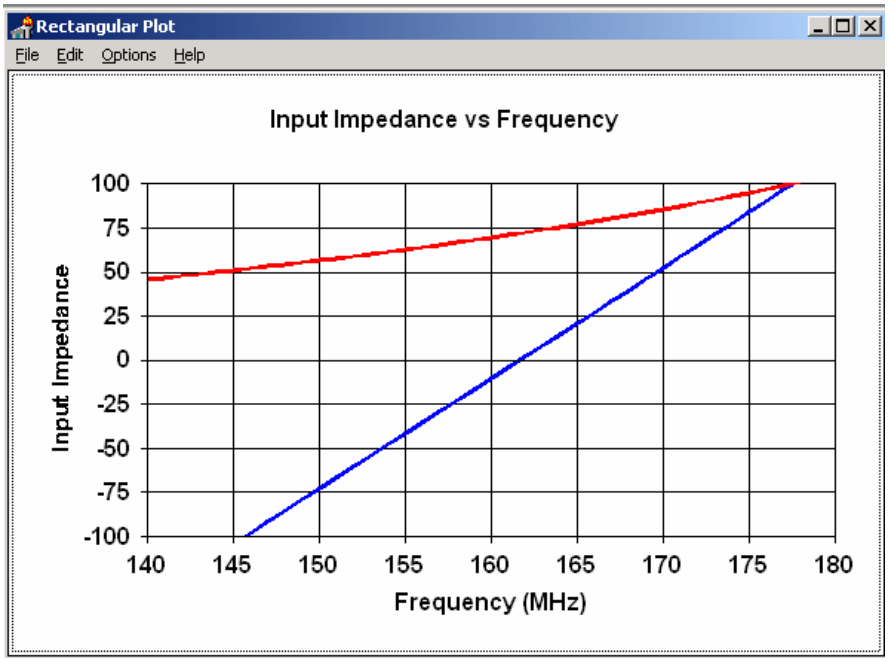

This validation ensures that the input impedance calculation is carried out correctly in XFDTD™, thereby enabling accurate estimates of the radiated power. It further ensures that the wire model employed in XFDTD™, which we used to model the antennas, produces physically meaningful current and fields distributions. Both these aspects ensure that the field quantities are correctly computed both in terms of absolute amplitude and relative distribution.

3) Computational parameters

a) The following table reports the main parameters of the FDTD model employed to perform our computational analysis:

PARAMETER	X	Y	Z
Voxel size	5 mm	5 mm	5 mm
Maximum domain dimensions employed for passenger computations with the trunk-mount antennas	425	1104	289
Maximum domain dimensions employed for bystander computations with the trunk-mount antennas	434	1243	580
Time step	Exactly equal to Courant limit (typically 10 *ps* at this frequency, with the body model)		
Objects separation from FDTD boundary (voxels)	>10	>10	>10
Number of time steps for passenger	Enough to reach at least -40 dB convergence		
Excitation	Sinusoidal (not less than 10 periods)		

4) Phantom model implementation and validation

a) The FDTD mesh of a male human body was created using digitized data in the form of transverse color images. The data is from the *visible human project* sponsored by the National Library of Medicine (NLM) and is available via the Internet (http://www.nlm.nih.gov/research/visible/visible_human.html). The male data set consists of MRI, CT and anatomical images. Axial MRI images of the head and neck and longitudinal sections of the rest of the body are available at 4 mm intervals. The MRI images have 256 pixel by 256 pixel resolution. Each pixel has 12 bits of gray tone resolution. The CT data consists of axial CT scans of the entire body taken at 1 mm intervals at a resolution of 512 pixels by 512 pixels where each pixel is made up of 12 bits of gray tone. The axial anatomical images are 2048 pixels by 1216 pixels where each pixel is defined by 24 bits of color. The anatomical cross sections are also at 1 mm intervals and coincide with the CT axial images. There are 1871 cross sections. The XFDTD™ High Fidelity Body Mesh uses 5x5x5 mm cells and has dimensions 136 x 87 x 397. Dr. Michael Smith and Dr. Chris Collins of the Milton S. Hershey Medical Center, Hershey, Pa, created the High Fidelity Body mesh. Details of body model creation are given in the *methods* section in [5]. The body mesh contains 23 tissues materials. Measured values for the tissue parameters for a broad frequency range are included with the mesh data. The correct values are interpolated from the table of measured data and entered into the appropriate mesh variables. The tissue conductivity and permittivity variation *vs.* frequency is included in the XFDTD™ calculation by a multiple-pole approximation to the Cole-Cole approximated tissue parameters reported by Camelia Gabriel, Ph.D., and Sami Gabriel, M. Sc. (http://www.brooks.af.mil/AFRL/HED/hedr/reports/dielectric/home.html).

a) The XFDTD™ High Fidelity Body Mesh model correctly represents the anatomical structure and the dielectric properties of body tissues, so it is appropriate for determining the highest exposure expected for normal device operation.

b) One example of the accuracy of XFDTD™ for computing SAR has been provided in [6]. The study reported in [6] is relative to a large-scale benchmark of measurement and computational tools carried out within the IEEE Standards Coordinating Committee 34, Sub-Committee 2.

5) Tissue dielectric parameters

a) The following table reports the dielectric properties used by XFDTD™ for the 23 body tissue materials in the High Fidelity Body Mesh at 450 MHz.

#	Tissue	ε_r	σ (S/m)	Density (kg/m^3)
1	skin	41.5	0.57	1125
2	tendon, pancreas, prostate, aorta, liver, other	50.3	0.76	1151
3	fat, yellow marrow	5.02	0.05	943

4	cortical bone	13.4	0.11	1850
5	cancellous bone	21.0	0.23	1080
6	blood	57.2	1.72	1057
7	muscle, heart, spleen, colon, tongue	63.5	0.99	1059
8	gray matter, cerebellum	54.1	0.88	1035.5
9	white matter	39.7	0.54	1027.4
10	CSF	68.9	2.32	1000
11	sclera/cornea	54.4	1.04	1151
12	vitreous humor	68.3	1.56	1000
13	bladder	17.6	0.31	1132
14	nerve	35.5	0.50	1112
15	cartilage	43.4	0.66	1171
16	gall bladder bile	76.5	1.62	928
17	thyroid	59.8	0.82	1035.5
18	stomach/esophagus	74.4	1.13	1126
19	lung	52.8	0.72	563
20	kidney	57.0	1.16	1147
21	testis	65.2	1.13	1158
22	lens	51.9	0.71	1163
23	small intestine	73.7	2.07	1153

Similarly, the table below reports the tissue dielectric properties at 155 MHz (mid-band for this VHF mobile radio product).

#	Tissue	ε_r	σ (S/m)	Density (kg/m^3)
1	skin	50.5	0.49	1125
2	tendon, pancreas, prostate, aorta, liver, other	59.3	0.63	1151
3	fat, yellow marrow	5.8	0.04	943
4	cortical bone	15.5	0.08	1850
5	cancellous bone	26.0	0.17	1080
6	blood	64.5	1.65	1057
7	muscle, heart, spleen, colon, tongue	73.6	0.84	1059
8	gray matter, cerebellum	71.5	0.73	1035.5
9	white matter	51.4	0.41	1027.4
10	CSF	73.9	2.29	1000
11	sclera/cornea	61.8	0.94	1151
12	vitreous humor	68.6	1.52	1000
13	bladder	19.1	0.28	1132
14	nerve	44.0	0.41	1112
15	cartilage	53.8	0.53	1171
16	gall bladder bile	86.6	1.49	928
17	thyroid	65.9	0.71	1035.5
18	stomach/esophagus	78.5	1.03	1126
19	lung	52.3	0.59	563

20	kidney	72.9	1.02	1147
21	testis	72.6	0.99	1158
22	lens	57.3	0.61	1163
23	small intestine	89.5	1.85	1153

b) The tissue types and dielectric parameters used in the SAR computation are appropriate for determining the highest exposure expected for normal device operation, because they are derived from measurements performed on real biological tissues (http://www.brooks.af.mil/AFRL/HED/hedr/reports/dielectric/home.html).

c) The tabulated list of the dielectric parameters used in phantom models is provided at point 5(a). As regards the device (car plus antenna), we used perfect electric conductors.

6) Transmitter model implementation and validation

a) The essential features that must be modeled correctly for the particular test device model to be valid are:

- Car body. We developed one very similar to the car used for MPE measurements, so as to be able to correlate measured and simulated field values. The model was imported in XFDTD™ from a CAD model that is commercially available at http://www.3dcadbrowser.com/
- Antenna. We used a straight wire, even when the gain antenna has a base coil for tuning. All the coil does is compensating for excess capacitance due to the antenna being slightly longer than half a wavelength. We do not need to do that in the model, as we used normalization with respect to the net radiated power, which is determined by the input resistance only. In this way, we neglect mismatch losses and artificially produce an overestimation of the SAR, thereby introducing a conservative bias in the model. In case of low profile vertical monopole antenna (HAE6016A) which has an additional horizontal metal circular disk at the tip, the disk was included in the model and well represented in 5 mm resolution mesh.
- Antenna location. We used the same location, relative to the edge of the car trunk, the backseat, or the roof, used in the MPE measurements. The following pictures show a lateral and a perspective view of the whole model (XFDTD™ does not show wires in this type of view, that is why the antenna is not visible).

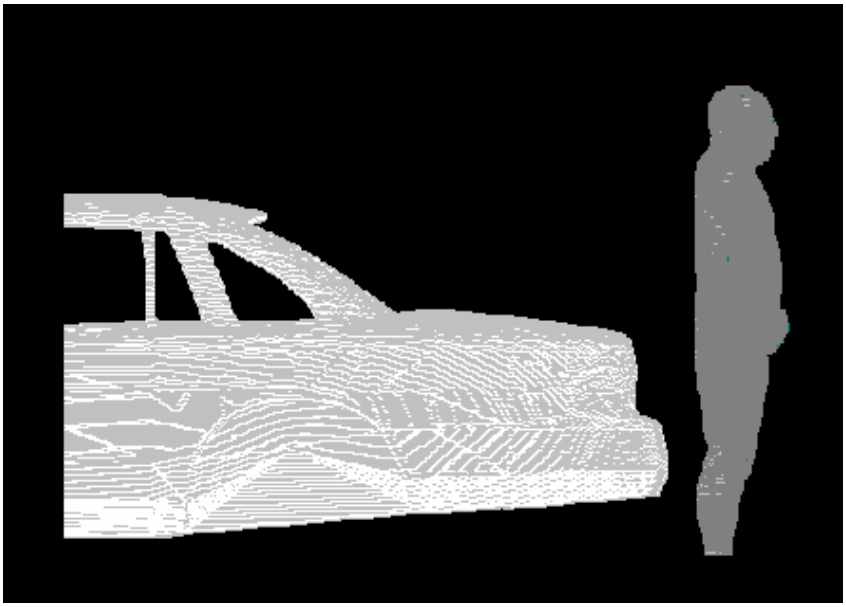

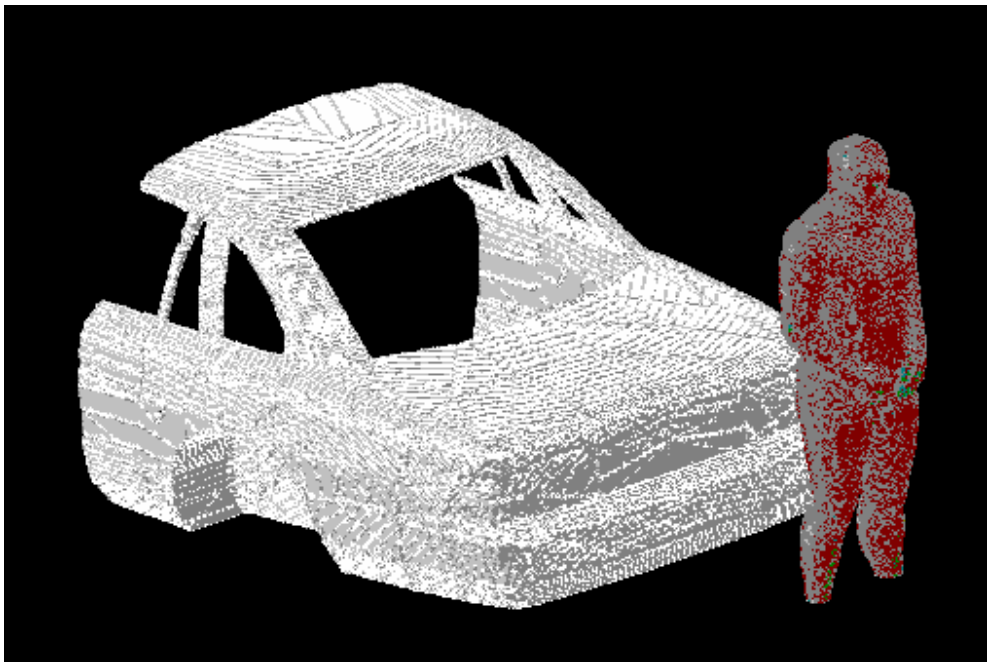

The car model is constituted by perfect electric conductor and does not include wheels in order to reduce its complexity. The passenger model is surrounded by air, as the seat, which is made out of poorly conductive fabrics, is not included in the computational model. The pavement has not been included in the model. The passenger and bystander models were validated for similar antenna and frequency conditions by comparing the MPE measurements at two VHF frequencies (146 MHz and 164 MHz) for antennas used for a VHF mobile radio analyzed previously in 2003 (FCC ID#ABZ99FT3046). The corresponding MPE measurements are reported in the compliance report relative to FCC ID#ABZ99FT3046. The comparison results are presented below, according to following definitions for the equivalent power densities (based on E or H-field):

$$S_E = \frac{|\mathbf{E}|^2}{2\eta}, \quad S_H = \frac{\eta}{2}|\mathbf{H}|^2, \quad \eta = 377\ \Omega$$

Passenger with 17.5 cm monopole antenna (HAE4002A 421.5 MHz)

The following figure of the test model shows the car model, where the yellow dots individuate the back seat, as it can be observed from the other figure showing the cross section of the passenger. The comparison has been performed by taking the average of the computed steady-state field values at the six dotted locations, corresponding to the head, chest, and legs along the yellow dots line, and comparing them with the average of the MPE measurements performed at the head, chest and legs locations. Such a comparison is carried out at the same rms power level (22 W, including the 50% duty factor) used in the MPE measurements.

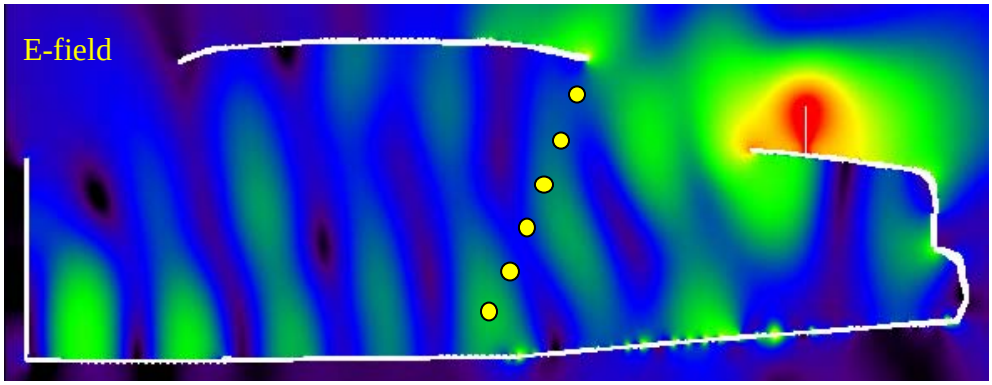

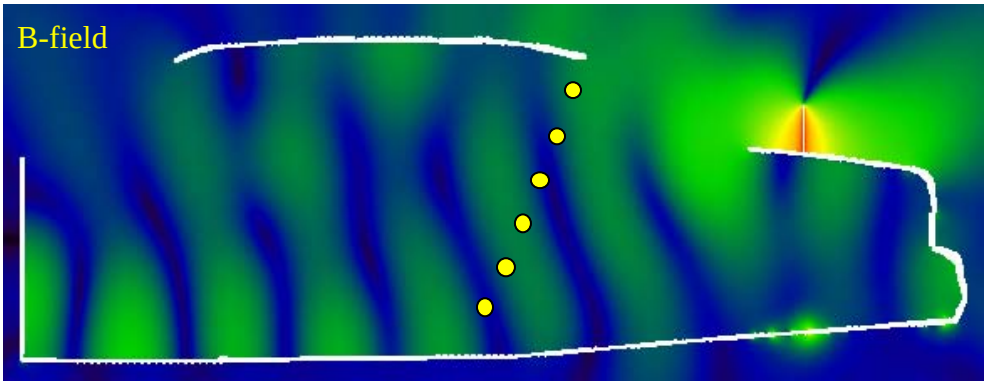

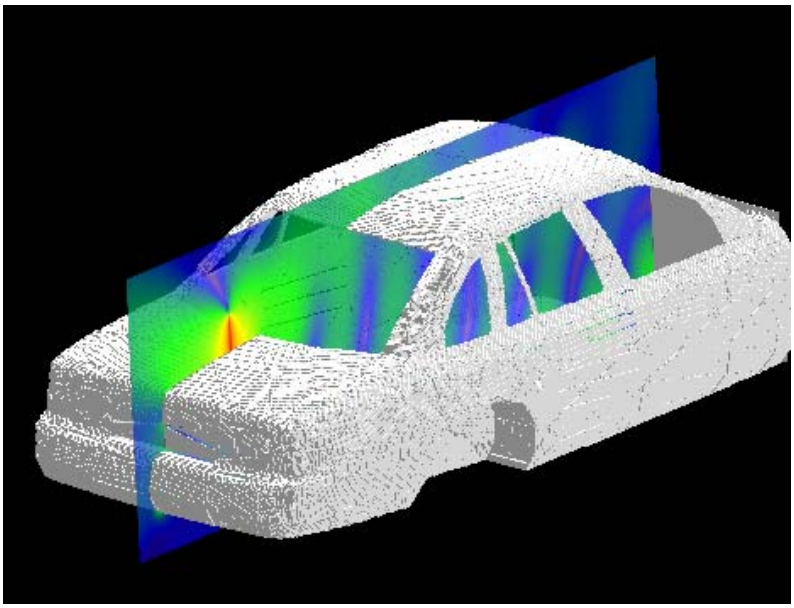

The equivalent power density (S) is computed from the E-field and the H-field separately. The following table reports the E-field values computed by XFDTD™ at the six locations, and the corresponding power density.

Location Number	E-field, V/m	Eq. Power Density 1.0 V source	Scaled Power Dens. 22 W output, mW/cm^2
1	5.83E-01	4.51E-04	4.41E-01
2	6.31E-01	5.28E-04	5.16E-01
3	6.50E-01	5.60E-04	5.48E-01
4	5.50E-01	4.01E-04	3.92E-01
5	4.50E-01	2.69E-04	2.63E-01
6	7.80E-01	8.07E-04	7.89E-01
Equivalent average Power Density			**4.92E-01**

Location Number	B-field, Weber/m2	Eq. Power Density 1.0 V source	Scaled Power Dens. 22 W output, mW/cm^2
1	2.26E-09	0.00061	5.96E-01
2	9.00E-10	0.00010	9.45E-02
3	1.20E-09	0.00017	1.68E-01
4	2.20E-09	0.00058	5.65E-01
5	1.90E-09	0.00043	4.21E-01
6	9.00E-10	0.00010	9.45E-02
Equivalent average Power Density			**3.23E-01**

The input impedance is 36.2+j24.8 ohm, therefore the radiated power (considering the mismatch to the 50 ohm unitary voltage source) is 2.25E-3 W, therefore a factor equal to 9779 is required to scale up to 22 W radiated. The corresponding scaled-up power densities are reported in the tables above, which show that the simulation overestimates the average power density from the MPE measurements (0.29 mW/cm^2), as derived from the measured E-field reported in the following table:

Position	SE (meas), 22 W output mW/cm^2
Head	0.38
Chest	0.33
Lower Trunk	0.16

The simulations tend to overestimate the average power density levels, which is understandable since there are no ohmic losses and perfect impedance matching is enforced in the computational models. Based on these results, we conclude that the simulation will produce slight exposure overestimates (about12%).

b) Descriptions and illustrations showing the correspondence between the modeled test device and the actual device, with respect to shape, size, dimensions and near-field radiating characteristics, are found in the main report.

c) Verification that the test device model is equivalent to the actual device for predicting the SAR distributions descends from the fact that the car and antenna size and location in the numerical model correspond to those used in the measurements.

d) The peak SAR is in the neck region for the passenger, which is in line with MPE measurements and predictions.

Passenger with 63.5 cm monopole antenna (HAE6010A 425 MHz)

The following figures show the car model with the field distribution in the horizontal planes where the MPE measurements have been performed. The comparison has been performed by taking the average of the computed steady-state field values at the three locations, corresponding to the head, chest, and lower trunk, and comparing them with the average of the MPE measurements performed at the head, chest and lower trunk locations. Such a comparison is carried out at the same rms power level (61.5 W, including the 50% duty factor) used in the MPE measurements.

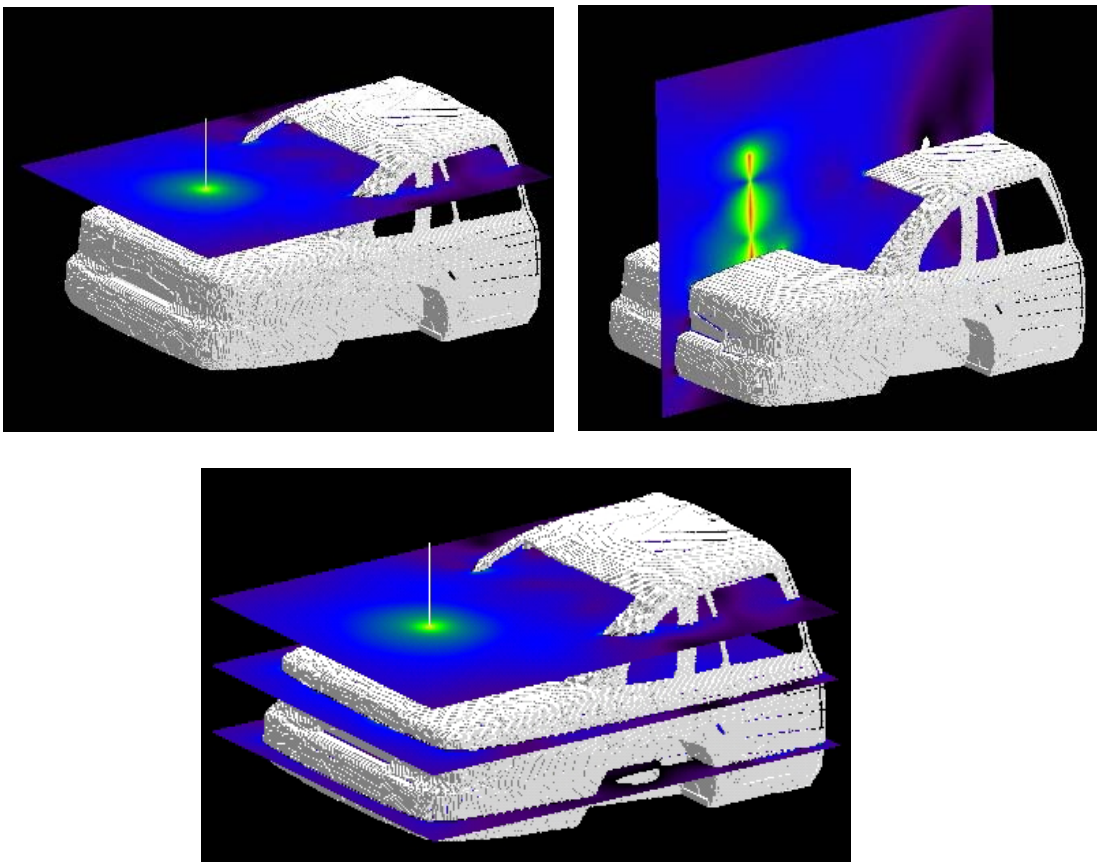

The equivalent power density (S) is computed from the E-field. The following table reports the E-field values computed by XFDTD™ at the three locations, and the corresponding power density.

Location Number	E-field, V/m	Eq. Power Density 1.0 V source	Scaled Power Dens. 61.5 W output, mW/cm^2
1	2.10E-01	5.85E-05	0.561
2	3.66E-01	1.78E-04	1.70
3	1.72E-01	3.92E-04	0.376
Equivalent average Power Density			**0.88**

The corresponding scaled-up power densities are reported in the tables above, which show that the simulation overestimates the average power density from the MPE measurements (0.52 mW/cm^2), as derived from the measured E-field reported in the following table:

Position	SE (meas), 60 W output mW/cm^2
Head	0.72
Chest	0.64
Lower Trunk	0.19

The simulations tend to overestimate the average power density levels, which is understandable since there are no ohmic losses and perfect impedance matching is enforced in the computational models. Based on these results, we conclude that the simulation will produce exposure overestimates (about 69%).

Bystander with 29 cm monopole antenna (HAE6013A 425 MHz)

The following figures show the E-field and H-field distributions across a vertical plane passing for the antenna and cutting the car in half. As done in the measurements, the MPE is computed from both E-field and H-field distributions, along the yellow dotted line at 10 points spaced 20 cm apart from each other up to 2 m in height. These lines and the field evaluation points are approximately indicated in the figures. The E-field and H-field distributions in the vertical plane placed at 90 cm from the antenna, behind the case, are shown as well. The points where the fields are sampled to determine the equivalent power density (S) are approximately indicated by the white dots. A picture of the antenna is not reported because it is identical to the HAE6013A.

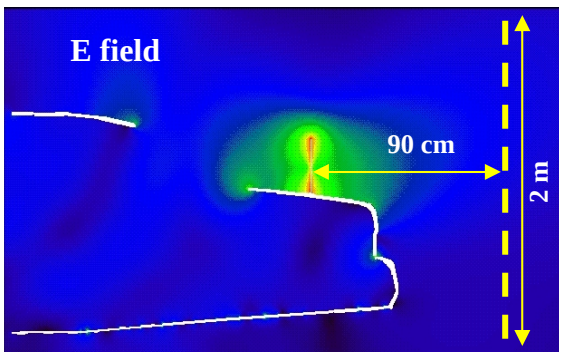

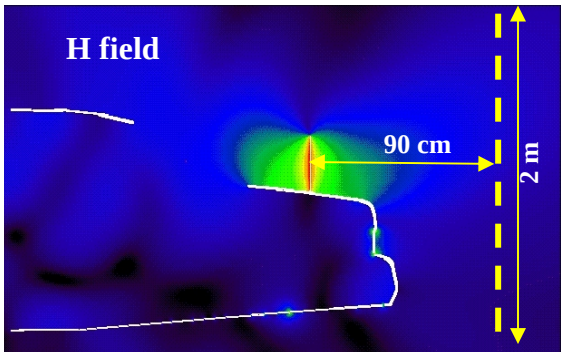

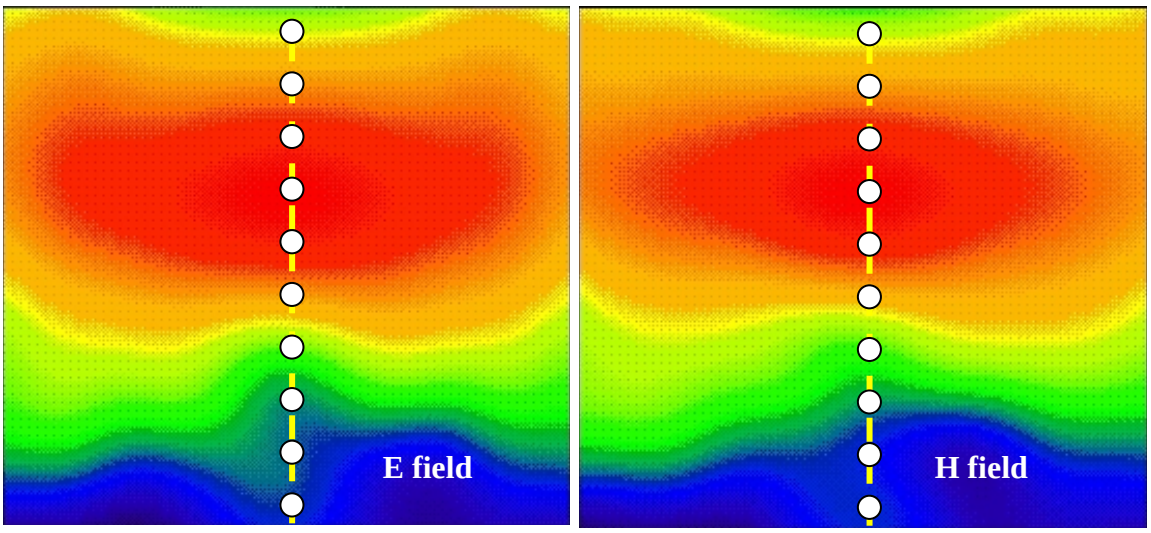

The following table reports the field values computed by XFDTD™ and the corresponding power density values. The average exposure levels are computed as well.

Height (cm)	E (V/m)	S_E (W/m^2)	H (A/m)	S_H (W/m^2)
0	1.05E-01	1.46E-05	2.90E-05	1.589E-05
20	1.14E-01	1.72E-05	2.90E-05	1.598E-05
40	1.16E-01	1.78E-05	3.14E-05	1.871E-05
60	1.39E-01	2.56E-05	3.75E-05	2.669E-05
80	2.03E-01	5.47E-05	5.03E-05	4.795E-05
100	2.73E-01	9.88E-05	7.23E-05	9.923E-05
120	2.94E-01	1.15E-04	8.17E-05	1.266E-04
140	2.65E-01	9.31E-05	7.32E-05	1.016E-04
160	2.12E-01	5.96E-05	5.73E-05	6.219E-05
180	1.60E-01	3.40E-05	4.32E-05	3.531E-05
Average S_E		**5.302E-05**	**Average S_H**	**5.501E-05**

Since the conducted power during the MPE measurement was 123 W the calculated power density was then scaled up for 61.5 W radiated power (taking into account 50% talk time). This model does not include the mismatch loss, loss in the cable and finite conductivity of the car surface and as represents a conservative model for exposure assessment. The scaled-up power density values for 61.5 W radiated power are 5.67 W/m^2 (E), and 5.88 W/m^2 (H), that correspond to 0.57 mW/cm^2 (E), and 0.59 mW/cm^2 (H). Measurements yielded average power density of 0.309 mW/cm^2 (E), which shows that the calculated power density is overestimated. The following graph shows a comparison between the measured power density and the simulated one, based on E or H fields, normalized to 61.5 W radiated power.

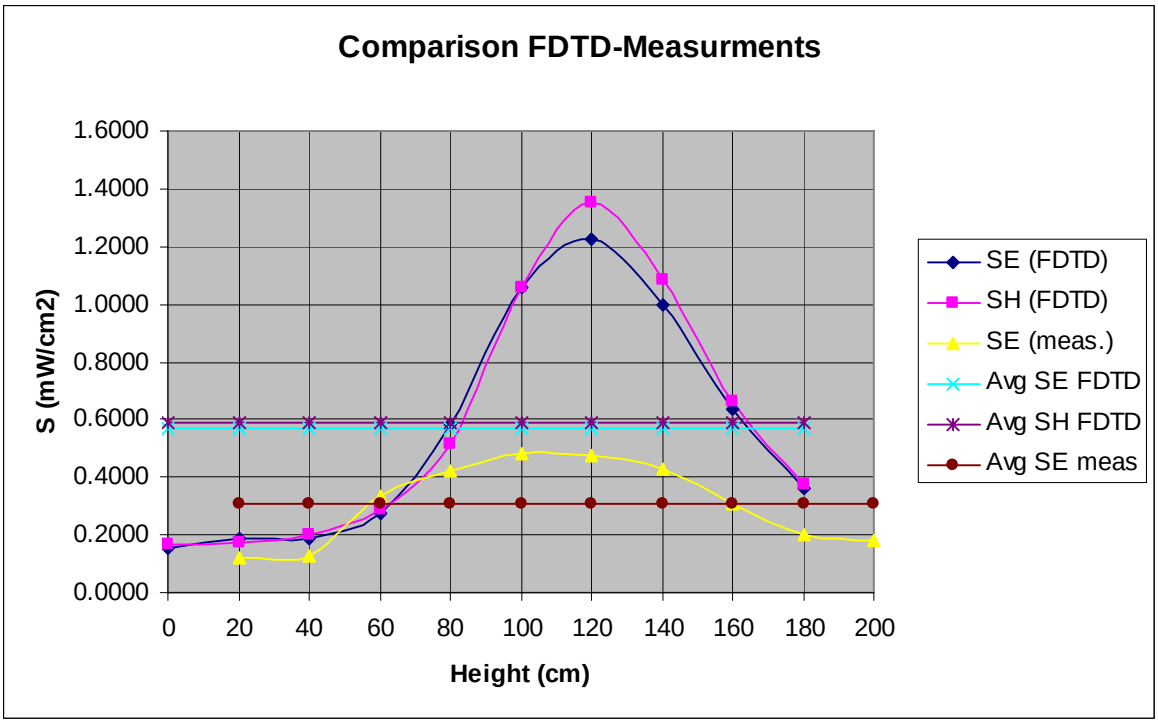

Bystander with 63.5 cm monopole antenna (HAE6010A 425 MHz)

The following figures show the E-field and H-field distributions across a vertical plane passing for the antenna and cutting the car in half. As done in the measurements, the MPE is computed from both E-field and H-field distributions, along the yellow dotted line at 10 points spaced 20 cm apart from each other up to 2 m in height. These lines and the field evaluation points are approximately indicated in the figures. The E-field and H-field distributions in the vertical plane placed at 90 cm from the antenna, behind the case, are shown as well. The points where the fields are sampled to determine the equivalent power density (S) are approximately indicated by the white dots. A picture of the antenna is not reported because it is identical to the HAE6010A.

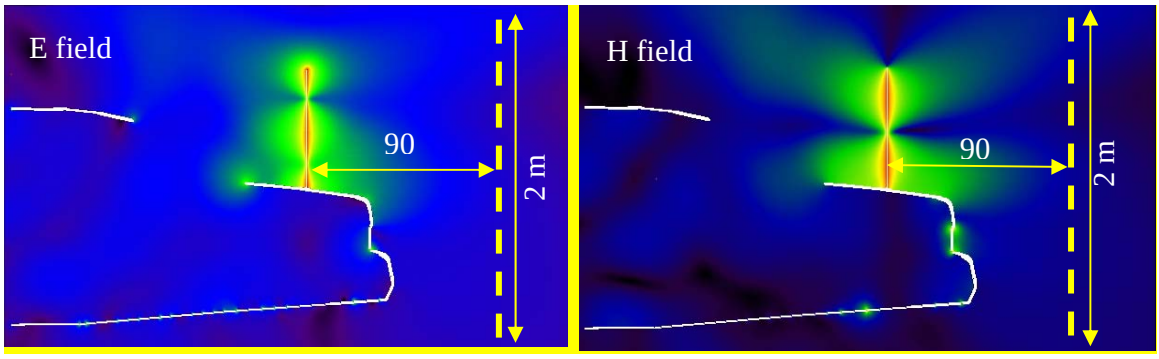

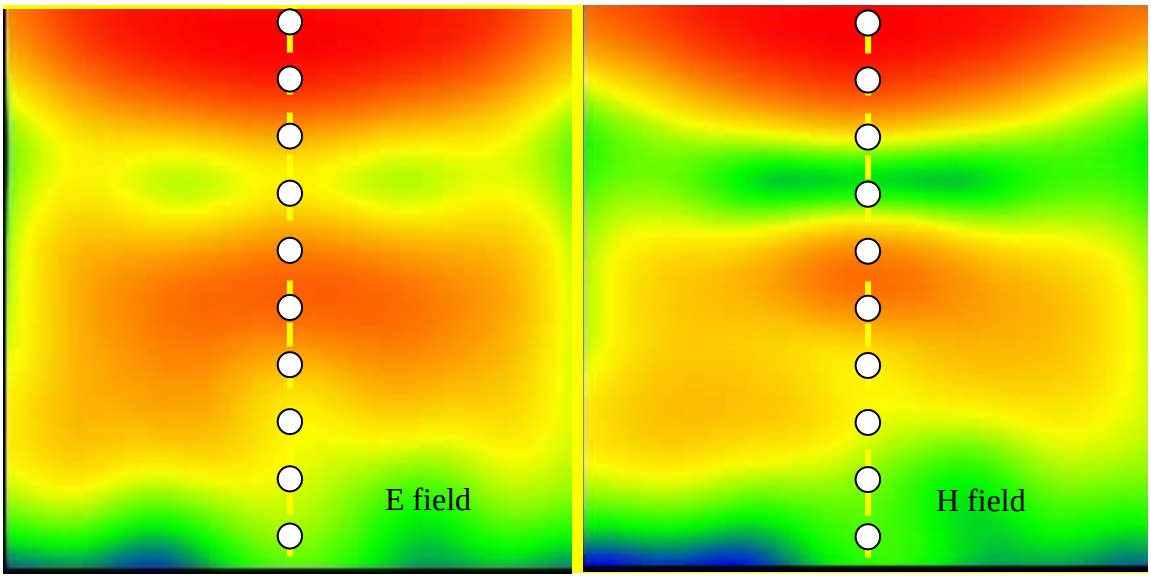

The following table reports the field values computed by XFDTD™ and the corresponding power density values. The average exposure levels are computed as well.

Height (cm)	E (V/m)	S_E (W/m^2)	H (A/m)	S_H (W/m^2)
0	1.32E-01	2.31E-05	4.51E-10	2.43E-05
20	1.49E-01	2.94E-05	4.82E-10	2.77E-05
40	1.58E-01	3.31E-05	5.44E-10	3.53E-05
60	1.71E-01	3.88E-05	5.79E-10	4.00E-05
80	2.10E-01	5.85E-05	6.78E-10	5.48E-05
100	2.12E-01	5.96E-05	7.60E-10	6.89E-05
120	1.67E-01	3.70E-05	4.86E-10	2.82E-05
140	1.83E-01	4.44E-05	5.57E-10	3.70E-05
160	2.50E-01	8.29E-05	8.62E-10	8.86E-05
180	2.68E-01	9.53E-05	9.75E-10	1.13E-04
Average S_E		**5.38E-05**	**Average S_H**	**5.18E-05**

Since the conducted power during the MPE measurement was 123 W the calculated power density was then scaled up for 61.5 W radiated power (taking into account 50% talk time). This model does not include the mismatch loss, loss in the cable and finite conductivity of the car surface and as represents a conservative model for exposure assessment. The scaled-up power density values for 61.5 W radiated power are 5.25 W/m^2 (E), and 5.06 W/m^2 (H), that correspond to 0.52 mW/cm^2 (E), and 0.51 mW/cm^2 (H). Measurements yielded average power density of 0.204 mW/cm^2 (E), which shows that the calculated power density is overestimated. The following graph shows a comparison between the measured power density and the simulated one, based on E or H

fields, normalized to 61.5 W radiated power.

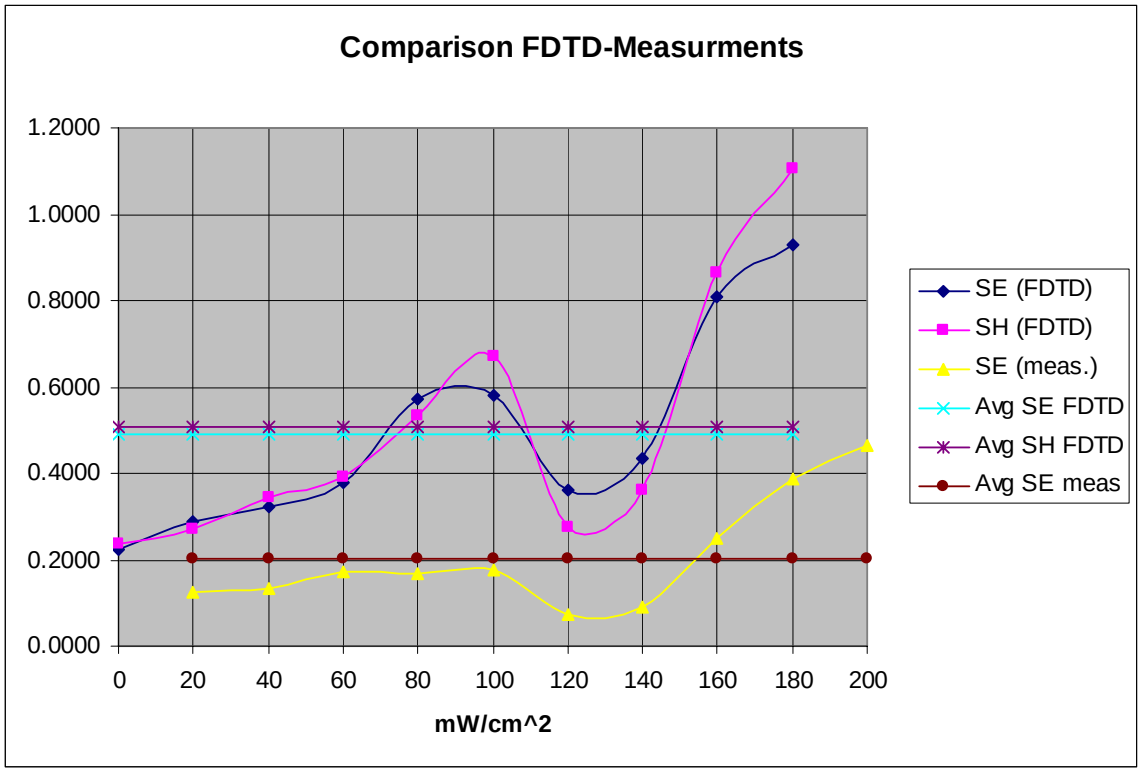

Passenger with 43 cm monopole antenna (HAD4009A 164 MHz)

The following figures of the test model show the empty car model, where the yellow dotted line represents the back seat, as it can be observed from the right-hand side figure showing the passenger. The comparison has been performed by taking the computed steady-state field values at the locations corresponding to the head, chest, and legs along the yellow line and comparing them with the corresponding measurements. Such a comparison is carried out at the same rms power level (56.5 W) used in the measurements. Steady-state E-field and H-field distributions at a vertical plane transverse to the car and crossing the passenger's head are displayed as well. Finally, a picture of the antenna is shown.

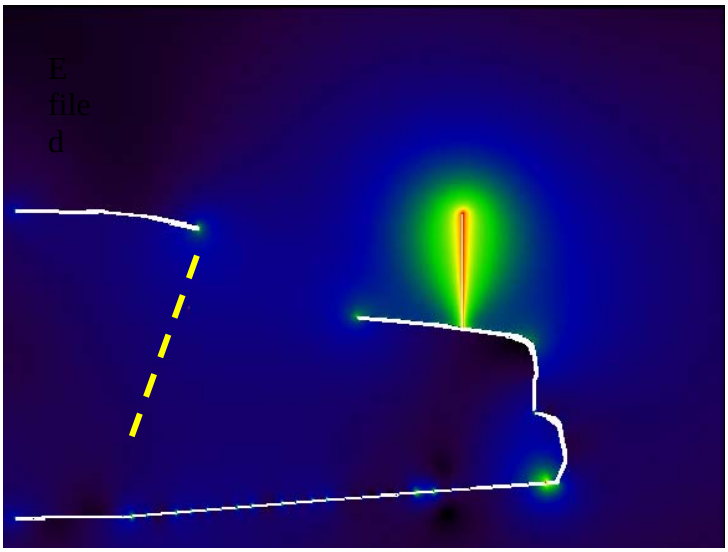

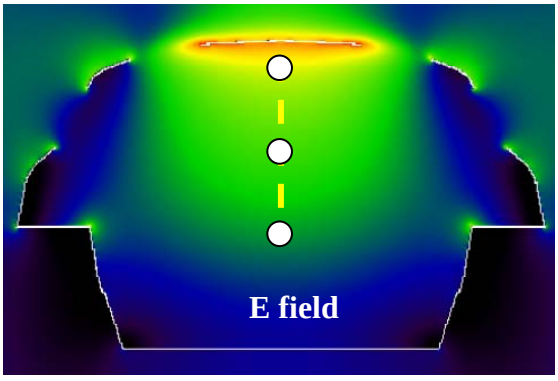

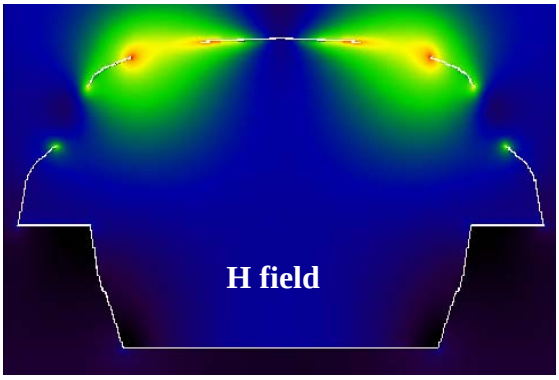

The highest exposure occurs in the middle of the backseat, which is also the case in the measurements. Therefore, the field values were determined on the yellow line centered at the middle of the backseat, approximately at the three locations that are shown by white dots. In actuality, the line is inclined so as to follow the inclination of the passenger's

back, as shown previously.

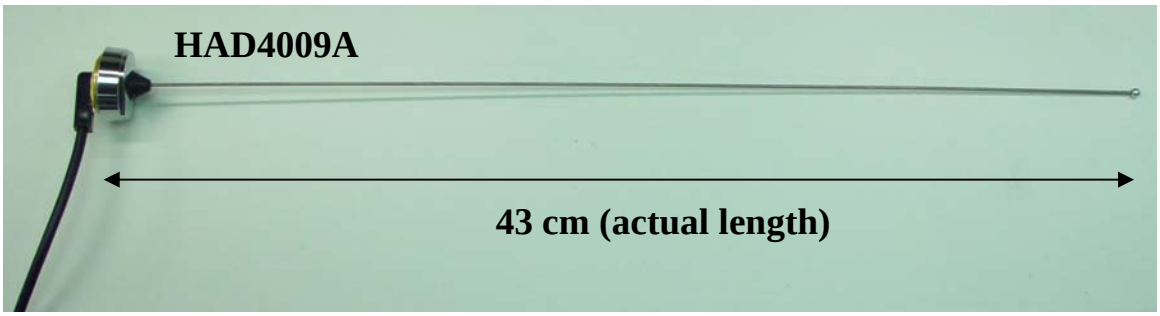

Because the peak exposure occurs in the center of the back seat, that was where we placed the passenger model to perform the SAR evaluations presented in the report. However, it can be observed that the H-field distribution features peaks near the lateral edges of the rear window. That is the reason why we also carried out one SAR computation by placing the passenger laterally in the back seat, in order to determine whether the SAR would be higher in this case.

As done in the measurements, the equivalent power density (S) is computed from the E-field, the H-field being much lower. The following table reports the E-field values computed by XFDTD™ at the three locations, and the corresponding power density.

Location	E-field magnitude (V/m)	S (W/m^2)
Head	1.10	1.33E-03
Chest	0.70	3.32E-04
Lower Trunk area	0.52	1.62E-04
	Average S	**6.07E-04**

The input impedance is 32.4-j4.8 ohm, therefore the radiated power (considering the mismatch to the 50 ohm unitary voltage source) is 2.38E-3 W. The scaled-up power density for 56.5 W radiated power is 14.4 W/m^2, corresponding to 1.44 mW/cm^2. Measurements gave an average of 1.29 mW/cm^2, which is in agreement considering conservativeness of simulations model. The following table and the graph show a comparison between the simulated power density and the measured one (see also MPE report in FCC ID#ABZ99FT3046, Table 43), normalized to 56.5 W radiated.

Position	SE (meas) mW/cm^2	SE (FDTD) mW/cm^2
Head	2.98	3.15
Chest	0.74	0.79
Lower Trunk	0.14	0.39

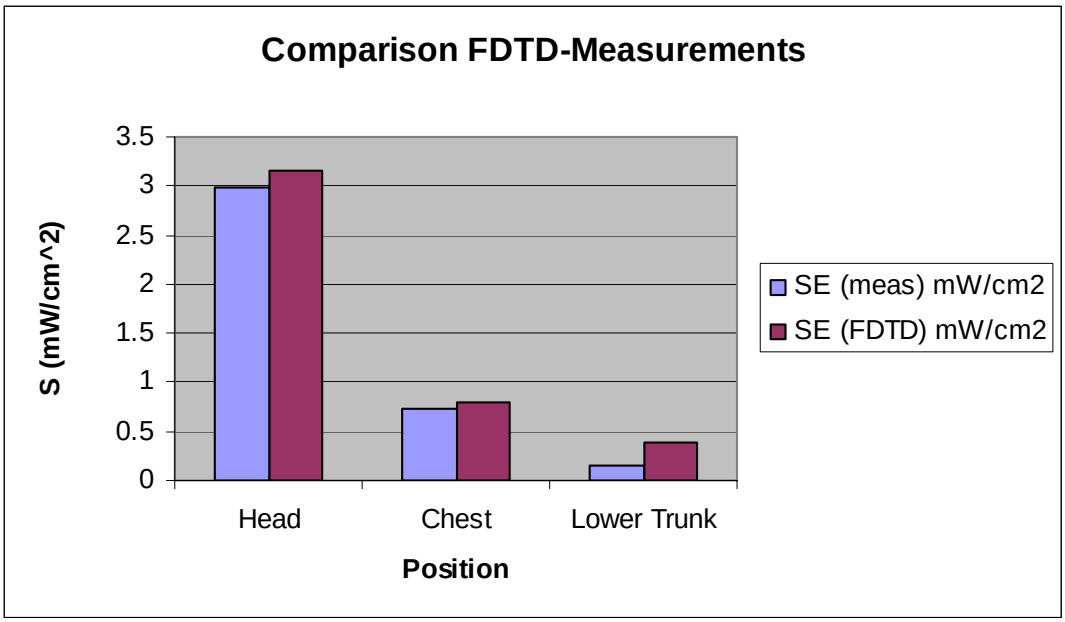

Bystander with 48 cm monopole antenna (HAD4007A 146 MHz)

The following figures show the E-field and H-field distributions across a vertical plane passing for the antenna and cutting the car in half. As done in the measurements, the MPE is computed from both E-field and H-field distributions, along the yellow dotted line at 10 points spaced 20 cm apart from each other up to 2 m in height. These lines and the field evaluation points are approximately indicated in the figures. The E-field and H-field distributions in the vertical plane placed at 60 cm from the antenna, behind the case, are shown as well. The points where the fields are sampled to determine the equivalent power density (S) are approximately indicated by the white dots. A picture of the antenna is not reported because it is identical to the HAD4009A except for the length.

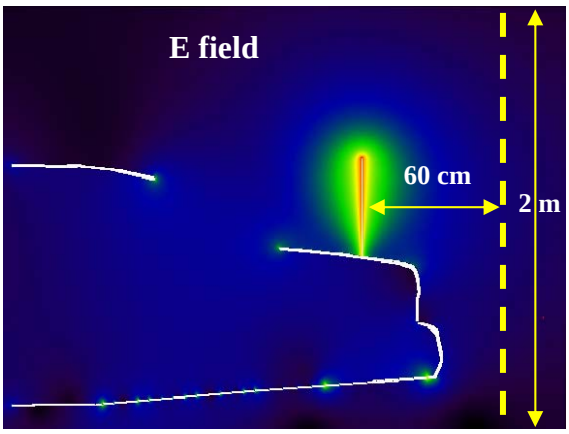

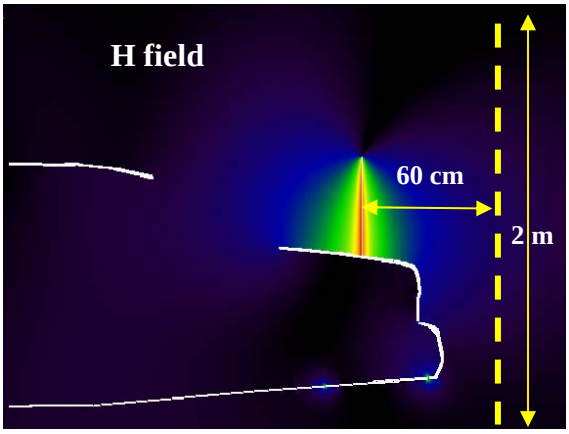

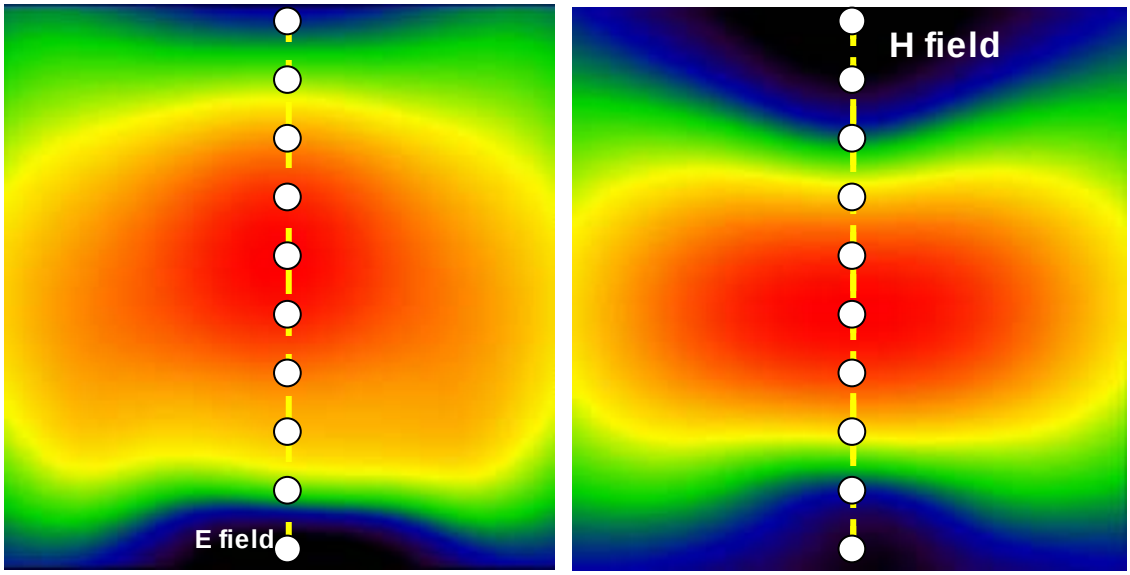

The following table reports the field values computed by XFDTD™ and the corresponding power density values. The average exposure levels are computed as well.

Height (cm)	E (V/m)	S_E (W/m^2)	H (A/m)	S_H (W/m^2)
20	2.12E-01	5.96E-05	5.21E-04	5.12E-05
40	3.86E-01	1.98E-04	8.59E-04	1.39E-04
60	4.48E-01	2.66E-04	1.36E-03	3.49E-04
80	5.36E-01	3.81E-04	1.77E-03	5.88E-04
100	6.17E-01	5.05E-04	1.88E-03	6.65E-04
120	6.32E-01	5.30E-04	1.61E-03	4.87E-04
140	5.65E-01	4.23E-04	1.15E-03	2.48E-04
160	4.47E-01	2.65E-04	7.21E-04	9.80E-05
180	3.30E-01	1.44E-04	4.07E-04	3.13E-05
200	2.35E-01	7.32E-05	1.93E-04	6.99E-06
	Average S_E	2.85E-04	**Average S_H**	2.66E-04

The input impedance is 27.9-j14.3 ohm, therefore the radiated power (considering the mismatch to the 50 ohm unitary voltage source) is 2.22E-3 W. The scaled-up power density values for 53.2 W radiated power are 6.81 W/m^2 (E), and 6.38 W/m^2 (H), that correspond to 0.68 mW/cm^2 (E), and 0.64 mW/cm^2 (H). Measurements yielded average power density of 0.664 mW/cm^2 (E), and 0.471 mW/cm^2 (H), i.e., which are in good agreement with the simulations. The following table and graph show a comparison between the simulated power density and the measured one, based on E (see MPE report in FCC ID#ABZ99FT3046, Table 1) or H fields (see MPE report in FCC ID#ABZ99FT3046, Table 13), normalized to 53.2 W radiated.

Height (cm)	SE (meas) mW/cm^2	SE (FDTD) mW/cm^2	SH (meas) mW/cm^2	SH (FDTD) mW/cm^2	Avg SE meas mW/cm^2	Avg SE FDTD mW/cm^2	Avg SH meas mW/cm^2	Avg SH FDTD mW/cm^2
20	0.19	0.14	0.2	0.12	0.664	0.681	0.471	0.638
40	0.37	0.47	0.23	0.33				
60	0.55	0.64	0.3	0.84				
80	0.68	0.91	0.56	1.41				
100	1.02	1.21	1.07	1.59				
120	1.15	1.27	1.1	1.17				
140	1.04	1.01	0.56	0.59				
160	0.79	0.63	0.24	0.23				
180	0.5	0.35	0.23	0.07				
200	0.35	0.18	0.22	0.02				

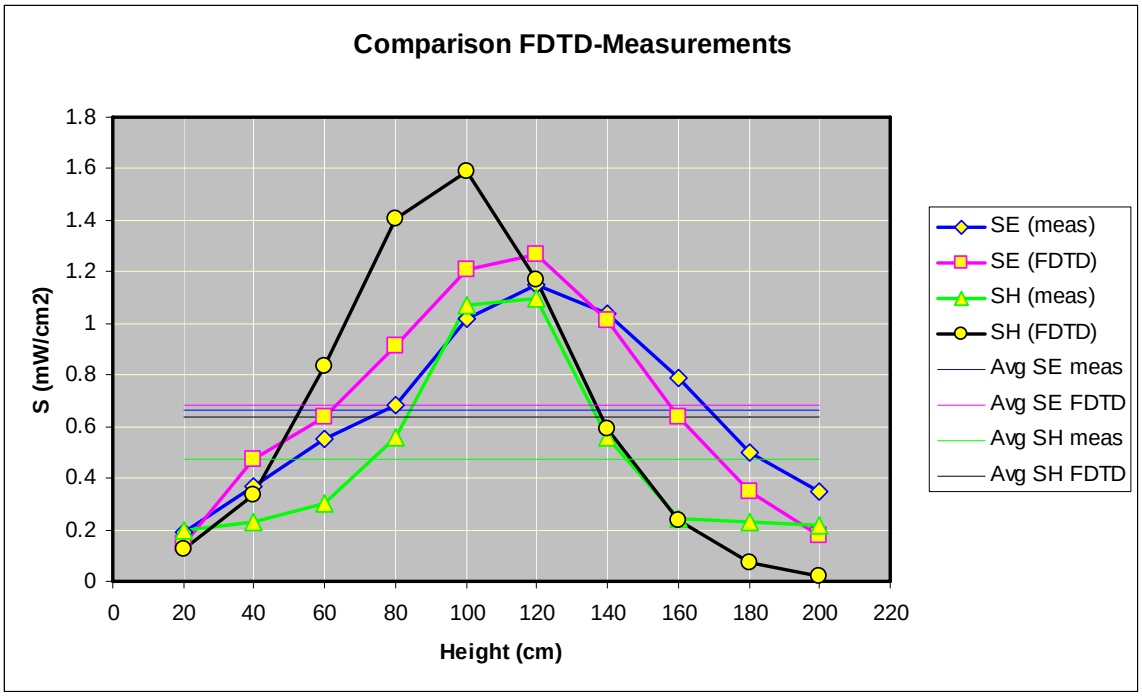

7) Test device positioning

a) A description of the device test positions used in the SAR computations is provided in the SAR report.

b) Illustrations showing the separation distances between the test device and the phantom for the tested configurations are provided in the SAR report.

8) Steady state termination procedures

a) The criteria used to determine that sinusoidal steady-state conditions have been reached throughout the computational domain for terminating the computations are based on the monitoring of field points to make sure they converge. The simulation projects were set to automatically track the field values throughout computational domain by means of XFDTD simulation control feature which ensures that "*convergence is reached when near-zone data shows a constant amplitude sine wave – when all transients have died down and the only variation left is sinusoidal. In this case "convergence" is tested on the average electric field in the space for its deviation from a pure sine wav. XFDTD automatically places points throughout the space for this purpose*." [XFDTD Reference Manual, version. 6.4]. This convergence threshold was set to -40 dB.
In addition for at least one passenger and one bystander exposure condition, we placed one "field sensor" near the antenna, others between the body and the domain boundary at different locations, and one inside the head of the model. In all simulations, isotropic E-field sensors were placed at opposite corners of the computational domain. We used isotropic E and H field "sensors", meaning that all three components of the fields are monitored at these points. The following figures show an example of the time waveforms at the field point sensors in the in two opposite points in the computational domain. We selected points near the lowest and highest grid index points. They are shown together in the figure. The highest field levels are observed for the higher index point, as it is closer to the antenna. In all cases, the field reaches the steady-state after a few cycles.

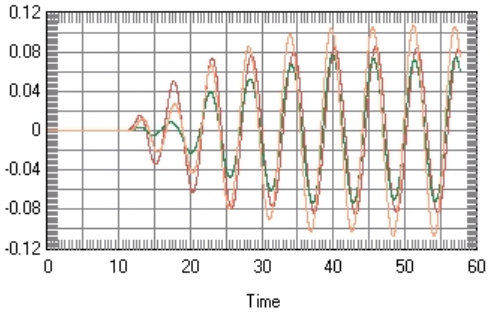

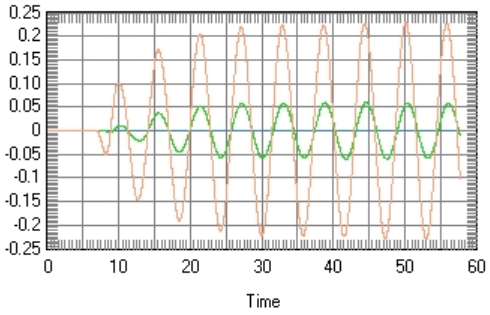

c) The XFDTD™ algorithm determines the field phasors by using the so-called "two-equations two-unknowns" method. Details of the algorithm are explained in [7].

9) Computing peak SAR from field components

a) The twelve E-field phasors at the edges of each Yee voxel are combined to yield the SAR associated to that voxel. In particular, the average is performed on the SAR values computed at the 12 edges of each voxel. Notice that in XFDTD™ the dielectric tissue properties are assigned to the voxel edges, thereby allowing said averaging procedure.

b) The IEEE Standards Coordinating Committee 34, Sub-Committee 2 draft standard P1529 (June 2000) discusses several algorithms for volumetric SAR averaging. It states that "It is observed that while the 12 components algorithm is the most appropriate from the mathematical point of view, the differences in 1g SAR calculated with either the 12 or 6 component methods are negligible for practical mesh resolutions (below 5mm). On the other hand, it is shown that the 3 components approach may lead to significant errors." XFDTD™ employs the 12-component method, which is the one recommended in the draft standard, thus providing the best achievable accuracy.

10) One-gram averaged SAR procedures

a) XFDTD™ computes the Specific Absorption Rate (SAR) in each complete cell containing lossy dielectric material and with a non-zero material density. To be considered a complete cell, the twelve cell edges must belong to lossy dielectric materials. The averaging calculation uses an interpolation scheme for finding the averages. Cubical spaces centered on a cell are formed and the mass and average SAR of the sample cubes are found. The size of the sample cubes increases until the total mass of the enclosed exceeds either 1 or 10 grams. The mass and average SAR value of each cube is saved and used to interpolate the average SAR values at either 1 or 10 grams. The interpolation is performed using two methods (polynomial fit and rational function fit) and the one with the lowest error is chosen. The sample cube must meet some conditions to be considered valid. The cube may contain some non-tissue cells, but some checks are performed on the distribution of the non-tissue cells. A valid cube will not contain an entire side or corner of non-tissue cells.

b) The sample cube increases in odd-numbered steps (1x1x1, 3x3x3, 5x5x5, etc) to remain centered on the desired cell. Since the visible human model employed herein has 5 mm resolution, the one-gram SAR is computed by averaging first over 1x1x1 voxels, corresponding to 0.125 cm^3 (not enough yet), and then over a 3x3x3 voxel cube, corresponding to about 3.4 cm^3, which is enough to include 1-g, and finally over a 5x5x5 voxel cube, corresponding to about 15.6 cm^3, which includes 10-g. The 1-g average SAR is computed by interpolating these three data points. This procedure is repeated in the surroundings of each voxel that is constituted by lossy materials, so as to determine the 1-g and/or 10-g SAR distributions.

c) As mentioned at points 10(a) and 10(b), the 1- gram average SAR is determined by interpolating the average SAR for the 1x1x1 , 3x3x3, and the 5x5x5 data points, corresponding to 0.125 cm^3, 3.4 cm^3, and 15.6 cm^3, respectively. Because the interpolation is carried out across three data points, the error introduced should be negligible because the interpolating curve crosses exactly the data points.

11) Total computational uncertainty – We derived an estimate for the uncertainty of FDTD methods in evaluating SAR by referring to [6]. In Fig. 7 in [6] it is shown that the deviation between SAR estimates using the XFDTD™ code and those measured with a compliance system are typically within 10% when the probe is away from the phantom surface so that boundary effects are negligible. In that example, the simulated SAR

always exceeds the measured SAR.

As discussed in 6(a), a conservative bias has been introduced in the model so as to reduce concerns regarding the computational uncertainty related to the car modeling, antenna modeling, and phantom modeling. The results of the comparison between measurements and simulations presented in 6(a) suggest that the present model produces an overestimate of the exposure between 4% and 36%. Such a conservative bias should eliminate the need for including uncertainty considerations in the SAR assessment.

12) Test results for determining SAR compliance

a) Illustrations showing the SAR distribution of dominant peak locations produced by the test transmitter, with respect to the phantom and test device, are provided in the SAR report.

b) The input impedance and the total power radiated under the impedance match conditions that occur at the test frequency are provided by XFDTD™. XFDTD™ computes the input impedance by following the method outlined in [8], which consists in performing the integration of the steady-state magnetic field around the feed point edge to compute the steady-state feed point current (*I*), which is then used to divide the feed-gap steady-state voltage (*V*). The net *rms* radiated power is computed as

$$P_{XFDTD} = \frac{1}{2}\mathrm{Re}\left\{VI^{*}\right\}$$

Both the input impedance and the net rms radiated power are provided by XFDTD™ at the end of each individual simulation.

We normalize the SAR to such a power, thereby obtaining SAR per radiated Watt (*normalized SAR*) values for the whole body and the 1-g SAR. Finally, we multiply such normalized SAR values times the max power rating of the device under test. In this way, we obtain the exposure metrics for 100% talk-time, i.e., without applying source-based time averaging.

c) For mobile radios, 50% source-based time averaging is applied by multiplying the SAR values determined at point 12(b) times a 0.5 factor.

REFERENCES

[1] K. S. Yee, “Numerical Solution of Initial Boundary Value Problems Involving Maxwell's Equations in Isotropic Media,” *IEEE Transactions on Antennas and Propagation*, vol. 14, no. 3, 302-307, March 1966.

[2] Z. P. Liao, H. L. Wong, G. P. Yang, and Y. F. Yuan, "A transmitting boundary for

transient wave analysis," Scientia Sinica, vol. 28, no. 10, pp 1063-1076, Oct. 1984.

[3] Validation exercise: Mie sphere. Remcom Inc. (enclosed PDF)


Remcom.pdf

[4] NEC-Win PRO ™ v 1.1, Nittany Scientific, Inc., Riverton, UT.

[5] C. M. Collins and M. B. Smith, "Calculations of B1 distribution, SNR, and SAR for a surface coil against an anatomically-accurate human body model," *Magn. Reson. Med.*, 45:692-699, 2001. (enclosed TIF)


Collins & Smith.pdf

[6] Martin Siegbahn and Christer Törnevik, “Measurements and FDTD Computations of the IEEE SCC 34 Spherical Bowl and Dipole Antenna,” Report to the IEEE Standards Coordinating Committee 34, Sub-Committee 2, 1998. (enclosed PDF)


Ericsson.pdf

[7] C. M. Furse and O. P. Gandhi, “Calculation of electric fields and currents induced in a millimeter-resolution human model at 60 Hz using the FDTD method with a novel time-to-frequency-domain conversion**,”** Antennas and Propagation Society International Symposium, 1996. (enclosed PDF)


Furse & Gandhi.pdf

[8] *The Finite Difference Time Domain Method for Electromagnetics*, Chapter 14.2, by K. S. Kunz and R. J. Luebbers, CRC Press, Boca Raton, Florida, 1993.